New whaitsioids (Therapsida: Therocephalia) from the Teekloof Formation of South Africa and therocephalian diversity during the end-Guadalupian extinction

Adam K. Huttenlocker Corresp., [1] , **Roger M. H. Smith** [2, 3]

[1] Department of Integrative Anatomical Sciences, University of Southern California

[2] University of the Witwatersrand, Evolutionary Studies Institute, Johannesburg, South Africa

[3] Iziko South African Museum, Cape Town, South Africa

Corresponding Author: Adam K. Huttenlocker
Email address: huttenlo@usc.edu

Two new species of therocephalian therapsids are described from the upper Permian Teekloof Formation of the Karoo Basin, South Africa. They include two specimens of a whaitsiid, *Microwhaitsia mendrezi* gen. et sp. nov., and a single, small whaitsioid *Ophidostoma tatarinovi* gen. et sp. nov., which preserves a combination of primitive and apomorphic features. A phylogenetic analysis of 56 therapsid taxa and 136 craniodental and postcranial characters places the new taxa within the monophyletic sister group of baurioids—Whaitsioidea—with *Microwhaitsia* as a basal whaitsiid and *Ophidostoma* as an aberrant whaitsioid just outside the hofmeyriid+whaitsiid subclade. The new records support that whaitsioids were diverse during the early-late Permian (Wuchiapingian) and that the dichotomy between whaitsiid-line and baurioid-line eutherocephalians was established early on. The oldest Gondwanan whaitsiid *Microwhaitsia* and additional records from the lower strata of the Teekloof Formation suggest that whaitsioids had diversified by the early Wuchiapingian and no later than *Pristerognathus* Assemblage Zone times. Prior extinction estimates based on species counts are reflected in an analysis of origination/extinction rates, which imply increasing faunal turnover from Guadalupian to Lopingian (late Permian) times. The new records support a growing body of evidence that some key Lopingian synapsid clades originated near or prior to the Guadalupian-Lopingian boundary ca. 260–259 million years ago, but only radiated following the end-Guadalupian extinction of dinocephalians and basal therocephalian predators (long-fuse model). Ongoing collecting in older portions of the Teekloof Formation (e.g., *Pristerognathus* Assemblage Zone) will shed further light on early eutherocephalians during this murky but critical time in their evolutionary diversification.

New whaitsioids (Therapsida: Therocephalia) from the Teekloof Formation of South Africa and therocephalian diversity during the end-Guadalupian extinction

ADAM K. HUTTENLOCKER[1,*] and ROGER M. H. SMITH[2,3]

[1] Department of Integrative Anatomical Sciences, University of Southern California, Los Angeles, California, U.S.A.;

[2]Evolutionary Studies Institute, University of the Witwatersrand, Johannesburg, South Africa;

[3]Iziko South African Museum, Cape Town, South Africa

*Corresponding author: *ahuttenlocker@gmail.com*

RH: HUTTENLOCKER & SMITH—TEEKLOOF WHAITSIOIDS

ABSTRACT—Two new species of therocephalian therapsids are described from the upper Permian Teekloof Formation of the Karoo Basin, South Africa. They include two specimens of a whaitsiid, *Microwhaitsia mendrezi* gen. et sp. nov., and a single, small whaitsioid *Ophidostoma tatarinovi* gen. et sp. nov., which preserves a combination of primitive and apomorphic features. A phylogenetic analysis of 56 therapsid taxa and 136 craniodental and postcranial characters places the new taxa within the monophyletic sister group of baurioids—Whaitsioidea—with *Microwhaitsia* as a basal whaitsiid and *Ophidostoma* as an aberrant whaitsioid just outside the hofmeyriid+whaitsiid subclade. The new records support that whaitsioids were diverse during the early-late Permian (Wuchiapingian) and that the dichotomy between whaitsiid-line and baurioid-line eutherocephalians was established early on. The oldest Gondwanan whaitsiid *Microwhaitsia* and additional records from the lower strata of the Teekloof Formation suggest that whaitsioids had diversified by the early Wuchiapingian and no later than *Pristerognathus* Assemblage Zone times. Prior extinction estimates based on species counts are reflected in an analysis of origination/extinction rates, which imply increasing faunal turnover from Guadalupian to Lopingian (late Permian) times. The new records support a growing body of evidence that some key Lopingian synapsid clades originated near or prior to the Guadalupian-Lopingian boundary ca. 260–259 million years ago, but only radiated following the end-Guadalupian extinction of dinocephalians and basal therocephalian predators (long-fuse model). Ongoing collecting in older portions of the Teekloof Formation (e.g., *Pristerognathus* Assemblage Zone) will shed further light on early eutherocephalians during this murky but critical time in their evolutionary diversification.

48 INTRODUCTION

49 Therocephalians were a major clade of nonmammalian therapsids whose fossils are best
50 represented in rocks of the middle to late Permian (ca. 272–251.9 million years ago), with a few
51 lineages that survived into the subsequent Triassic Period (Abdala et al., 2008; Huttenlocker et
52 al., 2011). They attained remarkable ecological diversity with wide-ranging body sizes and
53 myriad dental (and, thus, dietary) specializations and other modifications of their feeding
54 apparatus (Kemp, 1972a,b; Huttenlocker, 2014; Huttenlocker and Abdala, 2015; Huttenlocker et
55 al., 2015). Moreover, they are the sister group to cynodonts—the therapsid group that includes
56 mammals—making them exceptionally important in our understanding of the origins of
57 mammal-like behavior and physiology (Hopson and Barghusen, 1986; Hopson, 1991; van den
58 Heever, 1994; Huttenlocker, 2009). Thus, there has been increasing interest in therocephalian
59 paleobiology in recent years to clarify their evolutionary relationships (Huttenlocker, 2009;
60 Huttenlocker et al., 2011; Kemp, 2012) and to understand their fluctuating diversity patterns
61 within the context of the global biodiversity crises that disrupted terrestrial ecosystems of the late
62 Paleozoic—the end-Guadalupian and Permo-Triassic mass extinctions (Huttenlocker et al., 2011;
63 Huttenlocker, 2014).

64 Despite improvements in our understanding of therocephalian evolution, very little is
65 known about the transition between the middle-to-late Permian, a critical period in the ecological
66 expansion of therocephalians. Early therocephalian fossil localities are globally widespread—
67 particularly in present-day southern Africa and Russia—but their fossils are best known from the
68 middle Permian terrestrial vertebrate assemblages of the Karoo Basin, South Africa (Abdala et
69 al., 2008; Smith et al., 2012). Basal therocephalians of South Africa's middle Permian
70 (Guadalupian) *Tapinocephalus* and *Pristerognathus* assemblage zones (AZ) were large-bodied

apex predators that fell into only a handful of genera and species (Abdala et al., 2008; Abdala et al., 2014). By contrast, the later eutherocephalians that derived from this stock became highly diverse with up to 70 genera (Abdala et al., 2008; Huttenlocker, 2013), and abruptly replaced the earlier, archaic groups in the Karoo Basin by *Tropidostoma* AZ times. These eutherocephalians, along with the gorgonopsians, remained among the most abundant terrestrial predators in early-late Permian terrestrial assemblages in southern Africa (Smith & Botha-Brink, 2011; Smith et al., 2012). Moreover, a major dichotomy between baurioid-line and whaitsiid-line eutherocephalians may have already taken place prior to the early-late Permian *Tropidostoma* AZ, as some museum records of baurioid-line 'ictidosuchids' and whaitsiid-line hofmeyriids were collected from *Pristerognathus* AZ-equivalent rocks of the lower Teekloof Formation (reviewed in Huttenlocker, 2013 and this study).

Among Permian eutherocephalians, whaitsiids have received much taxonomic interest primarily due to the unconventional hypothesis that they may share a relationship with Cynodontia, thus positioning cynodonts within Therocephalia rather than as a close sister group (Kemp, 1972a; Abdala, 2007; Botha et al., 2007). Although this view has fallen out of favor (van den Heever, 1994; Kemp, 2012; Abdala et al., 2014), little remains known about the diversity of whaitsiid-line therocephalians or the detailed anatomy of their hypothetical common ancestor. The taxonomic history of whaitsioids is complex. Tatarinov (1974) was the first author to include his 'Annatherapsididae' (= Akidnognathidae), 'Moschowhaitsiidae,' and Whaitsiidae within the more inclusive clade 'Whaitsioidea.' However, Mendrez (1974a) separated from Whaitsiidae the akidnognathids and other forms that she did not see fit in either of the two groups, such as the hofmeyriids *Hofmeyria* and *Mirotenthes*—previously regarded as whaitsiids or "forerunners" of whaitsiids by Watson and Romer (1956:70) and other authors (e.g., Attridge,

1956; Brink, 1956). Early cladistic investigations of therapsids also doubted the whaitsiid affinities of akidnognathids and some hofmeyriids (Hopson and Barghusen, 1986; Abdala, 2007), although more recent revisions of therocephalian systematics and phylogeny have supported the traditional view that hofmeyriids likely do share a relationship with whaitsiids (Huttenlocker, 2009; Huttenlocker et al., 2011). Consequently, two major clades of post-akidnognathid eutherocephalians are currently recognized: (1) Baurioidea and (2) a clade of whaitsiids and hofmeyriids to which the term 'whaitsioids' has recently been repurposed (Huttenlocker et al., 2015; Huttenlocker and Sidor, 2016; Maisch, 2017) though it has not been formally defined until now.

Present Study— Here, we describe two new therocephalians from the western Karoo Basin that shed light on the poorly known nonmammalian therapsid subclade Whaitsioidea. These whaitsioid records were reported in prior studies (Sidor et al., 2013; Huttenlocker, 2014; Huttenlocker et al., 2015; Huttenlocker and Sidor, 2016), but their anatomy is described and illustrated here for the first time. The specimens were discovered in 1996 and 2011 on two different farms near the border of the Northern and Western Cape provinces, respectively, both from outcrops of the upper Permian Teekloof Formation (Fig. 1). Teekloof-equivalent rocks of the Middleton and lower Balfour formations to the east of the study area have yielded radiometric dates that suggest a relatively continuous sequence of middle to upper Permian rocks in this part of the basin (Rubidge et al., 2013). The combination of constraints on their early-late Permian ages (Wuchiapingian) coupled with their phylogenetic position near the whaitsiid stem makes these new records an important datum for understanding the post-Guadalupian radiation of eutherocephalians and of early nonmammalian therapsid faunas more generally.

GEOLOGICAL CONTEXT

The Beaufort Group is the most extensively exposed stratigraphic unit of the Karoo foreland basin sequence and consequently the most tetrapod fossils have been recovered from this interval. In the southwestern sub-basin, Beaufort Group sedimentation was initiated by source area tectonism and resulted in the deposition of an approximately 2,700 m thick succession of fluvial channel sandstones and overbank mudrocks (Abrahamskraal and Teekloof formations; Fig. 1) containing rich fossil tetrapod assemblages (i.e., *Eodicynodon, Tapinocephalus, Pristerognathus, Tropidostoma, Cistecephalus*, and *Daptocephalus* AZs of Fig. 1). Sandstone-rich fining-upward packages from 50 to 300 m thick, described as megacycles, occur within the succession. These packages are thought to be related to northeasterly, northwesterly, and east-southeasterly directed fluvial transport systems and subsidence-controlled shifts in the loci of channelization on the alluvial plain (Cole, 1992). The presence of calc-alkaline volcaniclastic detritus and cherts of tuffaceous origin suggests that the provenance rocks in the southwest may have included an active andesitic volcanic chain located on the eastern side of the Andean Cordillera in South America and West Antarctica. Rubidge et al. (2013) dated a series of these tuffs confirming that the Guadalupian-Lopingian boundary occurs close to the top of the Abrahamskraal Formation (Fig.1).

The overlying Wuchiapingian-aged Teekloof Formation in which the new therocephalians were found was deposited by overbank flooding from meandering rivers of variable sinuosity draining an extensive alluvial plain sloping gently towards the northeast in the direction of the receding Ecca shoreline (Turner, 1978). Deposition occurred under semi-arid climatic conditions as evidenced by the presence of desiccation cracks, playa lake evaporite

deposits with desert-rose gypsum aggregates and pedogenic carbonate nodules and lenses (Smith, 1990, 1993). The irregular accretion topography and preferential preservation of upper flow regime plane beds and lower flow regime ripple cross-lamination within channel sand bodies (Smith, 1987) indicates a flood-dominated discharge regime and seasonal inundation of the floodplains resulting in rapid bone burial (Smith, 1993).

The two new therocephalian skulls (SAM-PK-K10984, SAM-PK-K10990) collected from Badshoek (De Hoop 17) are from the same mudrock interval in the middle of the Hoedemaker Member (*Tropidostoma* AZ, +/- 257 Mya). They were found as isolated skulls and were encrusted with a 2 mm-thick layer of pedogenically-precipitated micrite. Associated dicynodont taxa collected in the same strata include *Tropidostoma, Emydops, Pristerodon* and *Diictodon*, as well as a small gorgonopsian (see Table 1).

The Good Luck (Matjiesfontein 412) specimens (SAM-PK-K8516, SAM-PK-K8631) were collected from massive gray siltstone beds in the upper Oukloof Member (upper *Cistecephalus* AZ, +/- 255 Mya) along with several skulls and partial skeletons of *Cistecephalus*, *Oudenodon*, *Diictodon, Procynosuchus* and *Pareiasaurus* (see Table 1).

MATERIAL AND METHODS

The electronic version of this article in Portable Document Format (PDF) will represent a published work according to the International Commission on Zoological Nomenclature (ICZN), and hence the new names contained in the electronic version are effectively published under that Code from the electronic edition alone. This published work and the nomenclatural acts it contains have been registered in ZooBank, the online registration system for the ICZN. The

ZooBank LSIDs (Life Science Identifiers) can be resolved and the associated information viewed through any standard web browser by appending the LSID to the prefix http://zoobank.org/. The LSID for this publication is: urn:lsid:zoobank.org:pub:4D798F6D-74BC-4FE8-BA46-79DAA314FE09. The online version of this work is archived and available from the following digital repositories: PeerJ, PubMed Central and CLOCKSS.

SYSTEMATIC PALEONTOLOGY

THERAPSIDA Broom, 1905

THEROCEPHALIA Broom, 1903

EUTHEROCEPHALIA Hopson and Barghusen, 1986

WHAITSIOIDEA Tatarinov, 1974

Composition—*Theriognathus microps* Owen, 1876; *Ictidostoma hemburyi* (Broom, 1911); *Hofmeyria atavus* Broom, 1935; *Ictidochampsa platyceps* Broom, 1948; *Mirotenthes digitipes* Attridge, 1956; *Moschowhaitsia vjuschkovi* Tatarinov, 1963; *Viatkosuchus sumini* Tatarinov, 1995; *Microwhaitsia mendrezi* gen. et sp. nov.; *Ophidostoma tatarinovi* gen. et sp. nov.

Definition—All eutherocephalians sharing a more recent common ancestry with *Theriognathus microps* and *Ictidostoma hemburyi*, than with *Ictidosuchus primaevus* and *Bauria cynops* [stem-based].

Revised diagnosis—Small- to large-bodied therocephalians having a wide suborbital bar forming well-frontated orbits; ventromedially infolded maxilla with medially positioned tooth

row so that much of the maxillary facial lamina is visible in ventral view; anterior border of orbit is located on anterior half of skull (conv. in cynodonts, *Lycosuchus*, some akidnognathids, and derived bauriamorphs); epipterygoid anteroposteriorly expanded; epipterygoid processus ascendens anterior edge orientation in lateral view is strongly anterodorsal (rather than posterodorsal or vertical) producing an anvil-shape; dentary tall and boomerang-shaped; and dentary ramus lateral groove weak (*Ophidostoma*) or absent (all others).

WHAITSIIDAE Haughton, 1918

Composition—*Theriognathus microps* Owen, 1876; *Ictidochampsa platyceps* Broom, 1948; *Moschowhaitsia vjuschkovi* Tatarinov, 1963; *Viatkosuchus sumini* Tatarinov, 1995; *Microwhaitsia mendrezi* gen. et sp. nov.

Definition—All eutherocephalians sharing a more recent common ancestry with *Theriognathus microps* than with *Ictidostoma hemburyi* and *Bauria cynops* [stem-based].

Revised diagnosis—Medium-to-large eutherocephalians with median frontonasal crest (also in *Chthonosaurus* and akidnognathids); suborbital vacuities reduced in size or absent; prefrontal and postorbital nearly contact, limiting contribution of frontal to dorsal border of orbit; epipterygoid extremely expanded anteroposteriorly (more so than hofmeyriids); epipterygoid posterior apophysis forms specialized “trigeminal notch”; pterygoid boss teeth usually absent (though present in *Viatkosuchus*).

MICROWHAITSIA MENDREZI gen. et sp. nov.

(Figs. 2-6)

209

210 **Etymology—***Micro* (Greek, 'small'); *whaitsia* (refers to whaitsiid affinities). Species
211 epithet honors Christiane Mendrez-Carroll for her substantial contributions to the morphology
212 and systematics of therocephalians.

213 **Holotype—**Iziko South African Museum (SAM) PK-K10990, partial skull with dentaries
214 preserved in occlusion, missing most of the braincase, occiput, and postdentary bones (Figs. 2–
215 4).

216 **Referred specimen—**SAM-PK-K10984, weathered snout preserving most of the left
217 antorbital region, palate, and maxillary canine and postcanine alveoli (Figs. 5–6).

218 **Locality and horizon—**Both specimens were collected by RMHS in 2011 from
219 Badshoek farm (De Hoop 117) near Beaufort West District, Western Cape Province, Republic of
220 South Africa; upper *Tropidostoma* Assemblage Zone (Wuchiapingian stage), upper Permian
221 Teekloof Formation (Hoedemaker member). Detailed locality information is available at Iziko
222 South African Museum, Cape Town.

223 **Diagnosis—**Small-to-medium sized therocephalian with broad, robust skull; nasals
224 strongly waisted at mid-length in dorsal view; thickened, pachyostotic frontal bone; thickened
225 suborbital bar (nearly as deep as the orbit dorsoventral height); upper dental formula
226 I5:pC1:C1:PC5; lower dental formula i4:c1:pc5.

227

228 **General**

229 In general, the two specimens of *Microwhaitsia* show a robust snout, cheek, and
230 dentition, and are similar to each other in overall size (estimated skull lengths ~180 mm). The
231 skull roofs are strongly sutured and craniofacial bones fairly thick for their small size. The

holotypic skull--SAM-PK-K10990--is nearly complete with dentition and both lower dentaries intact in occlusion, but it is missing much of the occiput and intertemporal region, as well as the postdentary bones. The referred specimen--SAM-PK-K10984--is a weathered snout and left antorbital region, missing the premaxilla, and most of the right side of the skull. The dentition is also missing from the referred specimen. In both specimens, cranial sutures are easily distinguished and tend to be noticeably sinuous and interdigitating, with few straight sutures except along the midline. The braincase and occiput are not preserved in either specimen.

Skull Roof

The premaxilla is a three-part element consisting of maxillary, vomerine, and dorsal (internarial) processes. The maxillary portion bears a short interdigitating suture with the maxilla that borders a small nervous foramen and, more dorsally, the septomaxillary foramen. Dorsally, the internarial process forms the medial septum of the naris and is fairly short, not reaching posteriorly beyond the level of the septomaxilla. The holotype preserves five premaxillary (incisor) alveoli. The septomaxilla is a rather large, solid element, but it is not well exposed outside of the naris. There is a modest dorsal process within the naris. The ventral footplate shares little overlap with the premaxilla externally, and the posterior facial process is fairly short dorsal and medial to the septomaxillary foramen.

The maxilla is the dominant element of the rostrum, having an exceptionally high facial lamina. The facial lamina is so high and broad and that very little of the nasal can be seen in lateral view (Figs. 2, 3). It is highest anteriorly and, when viewed laterally, rapidly tapers just behind the anterior border of the orbit ventral to the jugal. The lateral surface of the rostrum is coarsely pitted by many nervous foramina in front of the antorbital depression. In ventral (palatal) view, the maxilla borders a fossa for the lower canine and expands behind this area

forming a crista choanalis (Fig. 4). The crista is sufficiently expanded that it just contacts the vomer dorsally (Fig. 4B), separating the anterior (canine fossa) and posterior portions of the choana. However, there is no true maxillovomerine bridge as the connection is not sutural (unlike *Theriognathus* and *Moschowhaitsia* where the two elements are sutured). Attachment sites for maxilloturbinates on the medial side of the facial lamina could not be discerned.

The nasal is relatively long and narrow despite the broad, round profile of the snout. This is in part influenced by the large size of the maxilla facial laminae, which give the nasals a waisted appearance along their mid-length in dorsal view.

The lacrimal is a short, square element on the anterolateral margin of the orbit. It is much abbreviated due to the tall, broad facial lamina of the maxilla. Dorsally, it is bordered by the anterior tongue of the prefrontal, which contacts the maxilla and, thus, bars the lacrimal from contacting the nasal, as in most other therocephalians (except lycideopids). Just anterior to the orbit, near the contacts with the jugal and maxilla, there is a marked antorbital fossa which bears the lacrimal foramina (as in the therocephalian *Hofmeyria* and, convergently, burnetiamorph therapsids). One large foramen occupies a position on the anterior rim of the orbit, whereas the other smaller foramen is situated more ventrolaterally near the jugal-maxilla suture. The details of the nasolacrimal canal and its communication with the internal (medial) face of the maxilla could not be determined at present.

The prefrontal forms the anteromedial border of the orbit. It contacts the lacrimal ventrolaterally and the maxilla and nasal anteriorly. The posterior process does not contact the postorbital over the orbit, so that a small portion of the frontal contributes to the margin of the orbit. The prefrontal and postorbital nearly meet inside the orbit as in *Theriognathus* (Fig. 2C).

277 The frontal is very thick and pachyostotic (~13 mm thick at midorbit level). In dorsal
278 view, it is roughly diamond-shaped with stout lateral processes narrowly contacting the orbital
279 margin. The element's anterior extent just reaches the level of the anterior margin of the orbit
280 where it strongly interdigitates with the nasal. There is a prominent median frontonasal crest on
281 the midline as in other whaitsiids. The midline suture is comparatively straight except at the
282 midorbit level where it becomes noticeably jagged.
283 The postorbital bounds the posteromedial margin of the orbit. The postorbital bar is
284 robust and strongly sutures to the jugal. Most of the bar is formed by the broad postorbital
285 process of the jugal. As in *Theriognathus* and other whaitsiids, the jugal is a substantial element,
286 promoting the robust appearance of the skull despite its small size. However, the total depth of
287 the suborbital bar is more so than in other whaitsiid genera, being 40-50% the height of the skull
288 (nearly as tall as the orbit itself) (Figs. 2C, 3C). By contrast, hofmeyriids have comparatively
289 thin suborbital bars (e.g., *Hofmeyria*, *Mirotenthes*).
290 **Braincase and Occiput**
291 Most of the braincase and occiput are missing from the specimens. However, the bisected
292 referred specimen clearly shows portions of the sphenethmoid preserved in place. The
293 sphenethmoid complex has been described in a few therocephalians, including *Ictidosuchoides*
294 (Crompton, 1955), *Microgomphodon* (Abdala et al., 2014), *Tetracynodon* (Sigurdsen et al.,
295 2012), and *Theriognathus* (Kemp, 1972; Huttenlocker and Abdala, 2015). The anterodorsal
296 portion of the sphenethmoid complex, the orbitosphenoid, resides just dorsal and posterior to the
297 vomer, forming a broad but thin ascending lamina that would have made up the anteromedial
298 wall of the orbit. As in *Tetracynodon*, there is a broadly convex notch along its posterior margin

that may have accommodated the optic nerve (Sigurdsen et al., 2012: fig.2). Its dorsal most extent nearly contacts the ventral surface of the frontal, but is separated by a small fissure.

Palate, Splanchnocranium, and Suspensorium

The vomer is best viewed in palatal aspect in the holotype. It has a long interchoanal process that widens anteriorly as in other therocephalians and is widest at its anterior contact with the premaxilla. Although the crista choanalis just contacts the vomer anterodorsally, creating the appearance of a strongly vaulted palate, there is no true maxillovomerine bridge. There is a modest median crest that runs longitudinally along the vomer's ventral margin, and a suture that separates the vomer into right and left halves spans the entire posterior region and much of the length of the interchoanal process (as in basal therocephalians and some hofmeyriid specimens).

The crista choanalis is short and smoothly rounded, rolling onto the palatine and terminating just anterior to the suborbital vacuity. As in other whaitsiids, there are at least two prominent ridges formed in this region: one that is confluent with the vomer-palatine suture emarginating the choana and a second that is more laterally positioned and confluent with the palatine-maxilla suture and alveolar margin (Figs. 5B, 6B). The maxilla-palatine foramen is positioned somewhat posteriorly, just medial to the first and second postcanines. The ectopterygoid is preserved on the left side of the skull in the referred specimen. It formed a narrow strut bracing between the palatine, maxilla, and jugal along the anterolateral margin of the suborbital vacuity. It is pierced ventrally by a small foramen. Little of the pterygoid could be discerned in either specimen. Likewise, the epipterygoid and the suspensorium (including the quadrate-quadratojugal complex) are not preserved in either specimen.

Mandible

Portions of the left and right lower jaw are preserved in the holotypic specimen, including the left and right dentaries and splenials, right coronoid, right prearticular, and right surangular. The dentary was a robust element with a thick mentum that was only loosely sutured at the symphysis. The overall shape is strongly bowed as in other whaitsioids. The lateral surface of the ramus is smooth, bearing no dentary groove or trough. The anterior surface of the mentum is pitted with fine vascular foramina. The coronoid process was very tall, terminating in the upper half of the orbit, and its terminal margin was slightly rounded. On the medial surface of the dentary, a long, flat splenial can be seen running anteriorly and meeting on the left and right sides just behind the dentary symphysis. Just posterior and dorsal to the splenial on the right side, a single coronoid and anterior portions of the prearticular are preserved, bounding the anterior and lower parts of the mandibular fenestra. The anterior half of the surangular is preserved on the medial surface of the dentary coronoid process and forms the upper border of the mandibular fenestra. The majority of the postdentary region is unpreserved.

Dentition

The dentition is best preserved in the holotypic specimen, although maxillary alveoli are also present in the referred specimen. The holotype preserves five upper incisors, one upper precanine, one upper canine (a second root of a previously functional canine is also preserved on the left side of the skull immediately behind the newly functional canine), and five upper postcanines. The dentary preserves four lower incisors, a single lower canine, and five lower postcanines. As in most whaitsioids and early eutherocephalians in general, longitudinal fluting of the enamel was likely present on the incisors based on the fifth left upper incisor, which is the best preserved. However, most of the dentition is highly abraded, making the enamel texture

difficult to examine. In general, the incisor crowns are subcircular in cross-section and lack serrations or mesio-distal carinae. The upper canine is fairly large, subcircular in cross-section, and also lacks serrations or carinae. Following a short diastema, the postcanines are preserved as simple, conical crowns that are subcircular in cross-section. These also lack any serrations or mesio-distal carinae. The surface enamel of the postcanines is too poorly preserved to discern any postcanine fluting.

WHAITSIOIDEA incertae sedis

OPHIDOSTOMA TATARINOVI gen. et sp. nov.

(Figs. 7-8)

Etymology—Tatarinov's 'snake mouth.' *Ophido-* (Greek, 'snake' or 'serpent'); *stoma* (Greek, 'mouth'). Genus name refers to the wide gape permitted by the loose mandibular symphysis and streptostylic jaw of whaitsioid therocephalians. Species epithet honors Leonid Tatarinov for his contributions to whaitsioid systematics and therocephalian functional anatomy.

Holotype—SAM-PK-K8516, weathered skull and articulated, mandible missing portions of palate and braincase (Figs. 7–8).

Locality and Horizon—The specimen was collected by RMHS in 1996 on **'**Good Luck' farm (Matjiesfontein 412) near Fraserburg District, Northern Cape Province, Republic of South Africa; upper *Cistecephalus* Assemblage Zone (Wuchiapingian stage), upper Permian Teekloof Formation (Oukloof member). Detailed locality information is available at Iziko South African Museum, Cape Town.

366 **Diagnosis**—Small therocephalian with short, broad skull (greatest skull breadth at
367 occiput approximately equal to basal skull length); frontal length-to-width ratio approximately
368 1.0; pineal opening situated on raised boss; pterygoid boss teeth present; upper dental formula:
369 I?:C1:PC6. Plesiomorphic in retention of longitudinal striae/fluting on upper postcanines
370 (primitive for eutherocephalians).
371
372 **General**
373 The specimen consists of a small, poorly preserved skull and mandible (skull length from
374 occipital condyle to tip of snout ~60-65 mm), with the right side of the skull slightly crushed and
375 the lower jaw laterally displaced. Its most recognizable features are the stout rostrum and the
376 broad zygoma, producing a skull that is as wide as it is long.
377 The specimen was prepared using a pneumatic scribe so that most of the outer surface of
378 the skull roof and mandible was exposed, and the ventral surface prepared to the palate. The
379 skull was then scanned using high-resolution X-ray computed tomography (HRXCT) at the
380 University of Utah Core Imaging Facility to reveal aspects of the palate, cranial sinuses, and
381 braincase. It was scanned using an Inveon µ-CT scanner with scanner settings: 100 kV and 60
382 µA with a voxel size of 90 µm. Stacks were volumized and studied in OsiriX (Rosset et al.,
383 2004). Unfortunately, the HRXCT data revealed that much of the palate and basicranium was
384 'blown-out' prior to fossilization, leaving only the skull roof, peripheral portions of the braincase
385 and basicranium, and mandible.
386 The specimen has suffered from slight pre-burial distortion, including flaring of the right
387 cheek and loss of the right zygoma, allowing ventrolateral displacement of the dentary ramus,
388 although connection to the left dentary at the symphysis was maintained (Figs. 7D, 8D). The

squamosal is also displaced slightly anteriorly within the temporal fossa on both sides. This distortion has led the authors to consider the possibility that the striking breadth of the skull relative to its short length was a result of postmortem crushing or other deformation. However, these proportions likely did not result from preservational artifact because large portions of the skull roof are preserved in articulation and some *in situ* cranial calvariae are clearly broad with their widths being subequal to or slightly greater than their lengths (e.g., frontal).

Skull Roof

The maxilla is a very tall element with a broad facial lamina. The canine was deeply rooted, although it is mostly weathered and missing the entire crown. As in other whaitsioids, the facial lamina of the maxilla gently rolls onto the ventral (palatal) surface to meet the abbreviated alveolar margin (Figs. 7B, 8B). There are six closely packed postcanines situated along the alveolar margin on the right side of the skull. In palatal view, the choana can be seen to have been short and the crista choanalis also fairly short and rounded (rather than sharp medially). The medial surface of the facial lamina is smooth and shows no evidence for attachment of maxillary turbinates as in most other therocephalians (Huttenlocker et al., 2011; Sigurdsen et al., 2012; but see Hillenius, 1994). Internally, there is a large, cavern-like anterior maxillary sinus (sensu Sigurdsen, 2006) as in other therocephalians that have been serially sectioned or CT scanned (Sigurdsen et al., 2012). The sinus opens anteriorly onto the medial surface of the maxilla. A posterior duct parallels the tooth row, leading into a smaller sinus (the posterior maxillary sinus; sensu Sigurdsen, 2006) that opens posteriorly into a shallow fossa on the medial surface of the maxilla just behind the tooth row.

The nasals are imperfectly preserved in SAM-PK-K8516, with most of the left side weathered away and the right badly fractured. Surface features and nasoturbinal ridges could not

412 be discerned due to this damage. In life, the nasals would have been fairly short and broad as in
413 the other skull roof elements.

414 The lacrimal is a square element that forms part of the anterior wall of the orbit and
415 extends internally onto the palate. Two small nasolacrimal foramina located on the anterior
416 margin of the orbit open into the nasolacrimal canal. The canal forms a narrow caliber duct that
417 opens onto the medial surface of the facial lamina of the maxilla near the maxilla-lacrimal suture.

418 The prefrontal is a tall and broad element that forms most of the anteromedial margin of
419 the orbit. It is fairly fractured on the right side of the skull and slightly weathered on the left so
420 that its precise suture contacts are difficult to determine. However, given its breadth and the high
421 facial lamina of the maxilla, it is likely that it contacted the maxilla anteriorly so that a
422 nasolacrimal contact was not permissible as in most therocephalians.

423 The frontal forms a broad diamond that is as wide as it is long, a rare feature in a
424 therocephalian. The interorbital breadth is therefore relatively wider than in other
425 therocephalians. The dorsal surface is flat and smooth so that there is no median frontonasal
426 crest. The frontal contributes strongly to the dorsomedial wall of the orbit, widely separating the
427 prefrontal and postorbital. This contrasts with the condition in other whaitsioids where the latter
428 elements contact in the upper wall of the orbit (hofmeyriids) or nearly contact along its dorsal
429 margin (whaitsiids).

430 The postorbital is a lunate element forming most of the posterior border of the orbit. Its
431 jugal process is long and robust, although its connection to the jugal is not preserved due to
432 damage to the zygoma on both sides of the skull. More posteriorly, the postorbital broadly
433 overlaps the parietal extending beyond the level of the pineal foramen.

The jugal is incompletely preserved, forming only a portion of the ventrolateral margin of the orbit and missing the postorbital and zygomatic processes. Based on the preserved portions, the suborbital bar was very slender as in *Hofmeyria* and *Mirotenthes*. The squamosal is disarticulated on both sides of the skull, being displaced anteromedially into the temporal fossa. It is tall and thin with a broadly concave anterior face that, when articulated, overlapped the supraoccipital, interparietal, and parietal. The sutural overlap with the parietal was extensive as in the postorbital.

The parietal was a tall element forming the dorsolateral walls of the braincase, which were vertical and parallel-sided as in other eutheriodonts. The parietal (sagittal) crest was short behind the pineal foramen. Internally, the enclosure forming the pineal canal was deep and the external opening large and situated on an elevated parietal boss. The interparietal could not be discerned with certainty due to crushing in this region and anterior displacement of the supraoccipital.

Braincase and Occiput

Very little of the braincase and occiput are preserved in SAM-PK-K8516. The sphenethmoid complex could not be observed in the prepared specimen or in the CT scans. Small portions of the wedge-shaped supraoccipital are preserved on the left and right sides of the skull in close association with the parietal. Ventral to this, a tiny portion of the right exoccipital is preserved in contact with the basioccipital where the two would have bounded the foramen magnum. There was a strong basicranial girder formed between the ventromedian keel of the parabasisphenoid and the paired parasagittal processes of the pterygoid. The basal tubera are of moderate size (approximately 25% the width of the skull). The prootics and opisthotics are too poorly preserved to describe in detail.

Palate, Splanchnocranium, and Suspensorium

Much of the palate is unpreserved so that the relationships between the vomer, palatines and ectopterygoids cannot be described in detail. The maxillae bear a modest crista choanalis that border a fairly short choana. The crista is low and rounded, rather than sharp and distinct. Although the vomer is not preserved, a maxillovomerine bridge was likely to have been absent based on the lack of obvious medial (palatal) processes of the maxilla near the level of the canine or posterior to it. Portions of the pterygoid are preserved more posteriorly, showing well-developed transverse flanges that formed the posterior border of the suborbital vacuity. The flanges sweep medially and posteriorly where they formed paired parasagittal ridges bounding a wide interpterygoid vacuity. Pterygoid boss teeth are present, with three small, longitudinally arranged denticles present on the right and a large tooth preserved centrally on the left boss. The quadrate processes and the dorsally adjoining epipterygoid are not preserved. A massive element that rests within the quadrate recess of the squamosal on the left side of the skull is interpreted tentatively as the quadrate-quadratojugal complex.

Mandible

The mandible is preserved on the left and right sides of the skull. The left mandible is largely in place and held in occlusion, whereas the right is slightly ventrolaterally displaced and disarticulated. The dentary is long and strongly bowed, with the distinctive boomerang-shape that is common amongst whaitsioids. The coronoid process is broken on the left side, but is preserved on the right where it can be seen as an extremely tall element. This tall process would have terminated in the upper half of the temporal fenestra as in *Hofmeyria* and *Mirotenthes*. Its terminal margin is somewhat rounded. Along the ramus, there is a very modest lateral dentary groove (or trough), unlike in other whaitsioids that lack this feature entirely. Internally, there is a

large nervous canal that runs the length of the dentary, dorsal to the Meckelian groove, and feeds the alveoli. Medially, portions of the prearticular are preserved in contact with the Meckelian groove in the left side. The dentary, prearticular, and angular border a fairly large mandibular fenestra as in other eutherocephalians. The angular bears a broad but thin reflected lamina with radiating ridges and a dorsal notch. The surangular borders the reflected lamina dorsomedially. The presence of an articular in the specimen could not be confirmed.

Dentition

Due to damage to the premaxilla, the upper incisors are not preserved in the specimen. The upper canines were large and deeply rooted, although their crowns have also weathered away almost completely. Six postcanines are present in the right maxilla, although the roots of only three are preserved on the left. The crowns are short, conical with circular cross-sections and lacking carinae, and bear fine longitudinal striae on their external surface as in some basal akidnognathids (i.e., *Akidnognathus*) and baurioids (i.e., *Ictidosuchus*). Just anterior to the position of the second postcanine, a replacement tooth can be seen emerging from the maxilla on the right side.

Most of the lower incisors are missing, although a single pair of incisors (presumably in the fourth position) is preserved on both the left and right dentary, each pressed against the mesial surfaces of the lower canines. Their surface texture is abraded such that the presence of enamel striae (as in the postcanines) cannot be confirmed. The tooth row is very short with most of the teeth (including the postcanines) restricted to the anterior third of the dentary. There are at least four (and likely more) lower postcanines packed tightly together behind the lower canine. The anteriormost postcanine in the right dentary preserves enamel striae.

503 RESULTS & DISCUSSION

504

505 **Phylogenetic Position of New Whaitsioids**

506 Whereas early cladistic investigations regarded hofmeyriids as relatively basal
507 eutherocephalians (Hopson and Barghusen, 1986; Abdala, 2007), more recent studies have
508 supported that they are most closely related to whaitsiids, such as *Theriognathus* (Huttenlocker
509 and Abdala, 2015). Prior to the present study, the holotypic specimens of *Microwhaitsia* and
510 *Ophidostoma* were incorporated into a preliminary phylogenetic analysis and were referenced
511 only by their voucher numbers (Huttenlocker, 2014; Huttenlocker et al., 2015; Huttenlocker and
512 Sidor, 2016). We assessed the phylogenetic positions of *Microwhaitsia* and *Ophidostoma* using a
513 matrix of 136 craniodental and postcranial characters from 56 therapsid taxa (including two
514 outgroups *Biarmosuchus* and *Titanophoneus*, plus 54 neotherapsid ingroup taxa) (see
515 Supplementary Appendices S1 and S2). The data were analyzed in PAUP*4.0b10 (Swofford,
516 1999) and MrBayes v. 3.2.6 (Ronquist et al., 2009). A heuristic search was performed in PAUP
517 using maximum parsimony with a random addition sequence with 100 replicates and the tree-
518 bisection-reconnection (TBR) branch-swapping algorithm. Characters were not ordered and all
519 given equal weight. Multistate characters were interpreted as uncertainty. The Bayesian analysis
520 was performed using the standard Mk model for morphological evolution (Lewis, 2001) with
521 variable character rates. We ran the analysis for one million generations (with the first 25%
522 removed as burn-in) and sampled the posterior distribution every 100 generations.

523 Parsimony analysis recovered 1160 equally most parsimonious trees (MPTs) having a
524 length of 381 steps (consistency index (CI) = 0.438; retention index = 0.789; rescaled CI =
525 0.346). The analysis found Hofmeyriidae, Whaitsiidae, and Baurioidea to represent

monophyletic clades nested within Eutherocephalia. The high number of MPTs differed only in their volatile arrangements of basal scylacosaurid therocephalians, basal (ictidosuchid-grade) baurioids, and Triassic bauriids. Though the major (deep) branches of eutherocephalians are relatively stable, there were notable differences between parsimony and Bayesian-based approaches. In particular, the interrelationships of basal therocephalians are poorly resolved in the Bayesian topology, which fails to support the monophyly of Scylacosauridae. Moreover, the Bayesian topology yields a major eutherocephalian polytomy between Perplexisauridae, Chthonosauridae, Akidnognathidae, and the Whaitsioidea+Baurioidea clade. It also recovers the baurioid family Lycideopidae as the monophyletic sister group to Bauriamorpha, while the parsimony trees recover Lycideopidae as a paraphyletic assemblage that includes Bauriamorpha as a subgroup. To account for these uncertainties, we present a conservative topology in Figure 9 that illustrates the conflicting parsimony and Bayesian arrangements as polytomies.

All of the MPTs retrieved a monophyletic Whaitsiidae composed of the Permian eutherocephalians *Ictidochampsa* (Broom, 1948), *Viatkosuchus* (Tatarinov, 1995), *Moschowhaitsia* (Tatarinov, 1963), and *Theriognathus* (Owen, 1876). *Microwhaitsia* is found to be nested within whaitsiids as the sister taxon to *Viatkosuchus* + (*Moschowhaitsia* + *Theriognathus*). Among whaitsioids, characters shared between *Microwhaitsia* and other whaitsiids include: median frontonasal crest present; suborbital bar robust, deepened; postorbital bar moderately well built (extremely slender in hofmeyriids and baurioids); prefrontal and postorbital nearly contact on dorsomedial wall of orbit; upper postcanines reduced to five or fewer. Based on the character evidence, *Viatkosuchus* and *Microwhaitsia* would together represent the geologically oldest occurrences of whaitsiids in Laurasia and Gondwana, respectively (discussed further below).

549 *Ophidostoma* is found to be nested within Whaitsioidea, but the specimen does not
550 demonstrate clear anatomy that unites it with any given whaitsioid subgroup. Based on gross
551 similarities to hofmeyriids, Huttenlocker et al. (2015) labeled *Ophidostoma* as '*Cistecephalus*
552 AZ hofmeyriid' (Huttenlocker et al., 2015:fig. 6). However, the present analysis shows that
553 *Ophidostoma* falls outside the clade that includes the nearest common ancestor of
554 Hofmeyriidae+Whaitsiidae, indicating that it is an aberrant whaitsioid and that its hofmeyriid-
555 like gestalt represented plesiomorphies shared by all whaitsioids.

556 **Whaitsioidea-Baurioidea dichotomy—**The present phylogenetic hypothesis further
557 implies a major dichotomy between two non-akidnognathid eutherocephalian radiations during
558 the Permian: Whaitsioidea and Baurioidea. In general, the whaitsioids were characterized by
559 small and large-bodied species (skull lengths ranging ~6–35 cm) with a broad cranium having
560 greater area for the jaw adductor musculature, a robust, boomerang-shaped mandible, and a
561 tendency toward reduction of the postcanine teeth, whereas baurioids typically consisted of small
562 to mid-sized species (skull lengths ranging ~5–20 cm) with a low, slender rostrum and numerous
563 postcanines. A close relationship between whaitsioids and baurioids was originally demonstrated
564 by Huttenlocker (2009), who suggested that their common ancestry could be traced to no later
565 than the middle-to-late Permian transition during *Pristerognathus* AZ times.

566 Unlike Ivakhnenko's (2011) usage of 'Whaitsioidea' which included lycosuchids and
567 akidnognathids as subgroups—thus, making the name equivalent to Therocephalia—we define
568 Whaitsioidea explicitly as all eutherocephalians sharing a more recent common ancestry with
569 *Theriognathus microps* and *Ictidostoma hemburyi*, than with *Ictidosuchus primaevus* and *Bauria*
570 *cynops*. As such, the group includes representative hofmeyriid and whaitsiid taxa (e.g.,
571 *Hofmeyria*, *Theriognathus*), but excludes akidnognathids and baurioids. Permian whaitsioids

572 share a number of craniodental synapomorphies that distinguish them from the latter two groups,
573 including: a wide suborbital bar forming well-frontated (i.e., forward-facing) orbits;
574 ventromedially infolded maxilla facial lamina with concave alveolar margin (rather than convex
575 as in some akidnognathids, or straight as in all others); anterior border of orbit located on
576 anterior half of skull; anvil-shaped epipterygoid processus ascendens with anterior tilt (see
577 below); broad sutural contact between processus ascendens and parietal; dentary strongly bowed
578 or boomerang-shaped; dentary ramus lateral groove/furrow weak (*Ophidostoma*) to absent. Some
579 of these features have been discussed elsewhere (Huttenlocker, 2009; Huttenlocker et al., 2011).
580 Additional features of the braincase shared by whaitsioids may be elucidated with further
581 computed tomographic research. The external morphology of the whaitsioid braincase also
582 exhibits an anteriorly tilted epipterygoid with an anterodorsally oriented leading edge of the
583 processus ascendens (Figure 10) as demonstrated by a specimen of the hofmeyriid *Mirotenthes*
584 (SAM-PK- K11188) recovered from coeval *Cistecephalus* AZ deposits at 'Good Luck' in
585 association with *Ophidostoma*. This contrasts with the more upright or posteriorly leaning
586 epipterygoid of baurioids (e.g., Sigurdsen et al., 2012:fig. 2) and other therocephalians (e.g.,
587 Huttenlocker et al., 2011:fig. 4). The orientation of the processus ascendens has been
588 incorporated as new character 136 in the present phylogenetic analysis.

589 **Evolution of early eutherocephalian dental morphology and surface texture—**The
590 morphology and texture of the marginal dentition in therocephalians has only been discussed
591 anecdotally, but may provide important information regarding the interrelationships of
592 therocephalians, in addition to their diets (Huttenlocker et al., 2015). All eutherocephalians have
593 lost the serrations on the canines and antecanine teeth, but few eutherocephalians may have
594 retained smooth anterior and/or posterior carinae (e.g., chthonosaurids, some akidnognathids). In

595 some Permian eutherocephalians, the incisors and precanines may bear longitudinal fluting (e.g.,
596 basal akidnognathids, whaitsioids, and ictidosuchid-grade baurioids) or large, flat facets (derived
597 akidnognathids). Incisor fluting was suggested to be plesiomorphic for Eutherocephalia by
598 Hopson and Barghusen (1986), although the postcanine enamel texture was not discussed in any
599 detail. The condition of the incisors in *Ophidostoma* is unknown, but the presence of enamel
600 striae on the postcanines strongly suggests that striated postcanine enamel was also
601 plesiomorphic for the postcanines of early Eutherocephalia and its subclades, given its shared
602 presence in *Ophidostoma*, *Akidnognathus*, and *Ictidosuchus*. Incidentally, enamel fluting has also
603 been reported in the marginal dentition of the enigmatic scylacosaurian *Scylacosuchus* from
604 Russia (Ivakhnenko, 2011). Contrary to the recent suggestion of Huttenlocker et al. (2015:fig. 6)
605 that basal akidnognathids and ictidosuchid-grade baurioids evolved postcanine striae
606 independently, the new evidence from *Ophidostoma* suggests that a single evolutionary origin is
607 more parsimonious, followed by multiple losses of enamel fluting/striae on the antecanine teeth
608 and postcanines in derived Akidnognathidae, Whaitsioidea, and Baurioidea.
609

610 **Diversification of Therapsids during the End-Guadalupian Extinction**

611 Nonmarine vertebrate diversifications and extinctions are poorly understood during the
612 middle-to-late Permian transition. Particularly, whereas most workers recognize marked
613 extinctions of entire groups by the end of the Guadalupian (e.g., dinocephalians, lycosuchids,
614 scylacosaurids), there is little consensus as to whether the proliferation of late Permian therapsid
615 assemblages during Wuchiapingian times constitutes survival and opportunistic expansion of
616 ecospace by pre-existing lineages (long-fuse) or a rapid radiation of new lineages (short-fuse)
617 during the extinction's aftermath (Fröbisch, 2008, 2013; Lucas, 2017). For example, Lucas

(2017) most recently characterized the extinction of dinocephalian faunas as an abrupt "global event" (p. 55), although systematic paleontological collecting in the middle Permian *Tapinocephalus* and *Pristerognathus* AZs suggests the turnover was more complex, and that the apparent severity of dinocephalian extinctions is exaggerated by oversplit dinocephalian taxonomy and poor temporal resolution (Rubidge et al., 2013; Day et al., 2015a,b). Nevertheless, others have identified shifts in overall extinction rates of some post-Guadalupian therapsid lineages—a potential driver of apparent (raw) diversity shifts in some Wuchiapingian lineages (Brocklehurst et al., 2015)—while others still have raised doubts about the quality of the fossil record and its ability to resolve the magnitude of turnover of middle-to-late Permian assemblages (Fröbisch, 2008, 2013; Irmis et al., 2013).

We suggest that the apparent turnover of therocephalians can be characterized by a long-fuse model in which classic late Permian clades (e.g., whaitsioids, baurioids) originated concurrently with basal therocephalians of the middle Permian, but at lower abundances. This hypothesis is supported by renewed collecting efforts in the Teekloof Formation by one of us (RMHS), helping to further clarify therapsid ecological turnover during this time. Firstly, the new record of *Microwhaitsia* represents one of the oldest known Gondwanan whaitsiids, as other whaitsiid records from southern Africa are typically confined to the uppermost *Cistecephalus* and lower *Daptocephalus* AZs (Huttenlocker and Abdala, 2015). *Microwhaitsia* firmly establishes that whaitsiids already exhibited a Pangean-wide distribution by *Tropidostoma* AZ times (early Wuchiapingian), an observation that is consistent with the record of the closely allied *Viatkosuchus* from the Capitanian or Wuchiapingian-aged Kotelnich assemblage of Russia (Golubev, 2000; Benton et al., 2012) (Fig. 11). Secondly, long-term collecting efforts by one of us (RMHS) to elucidate the assemblages of the different members of the Teekloof Formation

641 have produced additional whaitsioid and baurioid records (see Tables 2 and 3). Some of these—
642 including a hofmeyriid (SAM-PK-K10525) (Fig. 12), an indeterminate ictidosuchid-grade
643 baurioid (SAM-PK-K6886) and a second baurioid with possible affinities to *Ictidosuchoides*
644 (SAM-PK-K11319)—were collected from the lower Poortjie Member or equivalent beds, which
645 contains a *Pristerognathus* AZ fauna that corresponds to either the latest Capitanian or earliest
646 Wuchiapingian global stages (Fig. 1).
647 Origination, extinction, and diversification rate shifts in therocephalians have been
648 summarized elsewhere in the context of the Permo-Triassic mass extinction (Huttenlocker et al.,
649 2011; Huttenlocker, 2013, 2014). For example, Huttenlocker (2014) failed to identify evidence
650 of diversification rate shifts in small-bodied therocephalian lineages near the Permo-Triassic
651 boundary, but noted a significant shift associated with the earlier divergence of the
652 Eutherocephalia clade. This was attributed to either increasing origination rates of
653 eutherocephalians or to sampling bias in the *Tropidostoma* and *Cistecephalus* AZs where
654 therocephalian fossils are more abundant (Smith et al., 2012). More recently, Brocklehurst et al.
655 (2015) showed that uneven origination and extinction rates (particularly elevated extinction)
656 could be a driver of diversification rate shifts in Permo-Triassic tetrapods. Notably, both
657 origination *and* extinction rates of therocephalians rose steadily into the late Permian (Fig. 11),
658 despite the long lineage durations sustained by a few representative taxa during the
659 Wuchiapingian (e.g., *Ictidosuchoides*, some hofmeyriids). In this sense, origination/extinction
660 rates indicate that therocephalians (particularly eutherocephalians) were, on the whole, resilient
661 to the effects of the extinction, although this was dependent upon high rates of turnover and
662 replacement by individual genera. Unlike some baurioid lineages, whaitsioids became wholly
663 extinct prior to the Permo-Triassic boundary as therocephalian origination rates began to

markedly decrease. The reasons for this differential extinction remain unclear, but have been linked to differences in life history strategies evident in the two groups (Huttenlocker and Botha-Brink, 2013, 2014; Botha et al., 2016). Consequently, future collecting of precious middle-to-late Permian specimens will be crucial to further resolve the evolutionary dynamics of therocephalians spanning the end-Guadalupian and Permo-Triassic mass extinctions.

CONCLUSIONS

The new records of *Microwhaitsia* and *Ophidostoma* from the Teekloof Formation shed light on the early evolution of eutherocephalians during the middle-to-late Permian transition. Phylogenetic analysis recovers both of the new taxa within Whaitsioidea, with *Microwhaitsia* as an early whaitsiid and *Ophidostoma* as an aberrant whaitsioid outside the hofmeyriid+whaitsiid clade. Consequently, *Microwhaitsia* represents the oldest whaitsiid from Gondwana and, along with additional early hofmeyriid and baurioid records, underscores the early dichotomy between whaitsiid-line and baurioid-line therocephalians. Moreover, the disjunct geographic occurrences of *Microwhaitsia* and *Viatkosuchus* suggest that whaitsiids already exhibited a cosmopolitan distribution by the early Wuchiapingian. During the end-Guadalupian, the extinction of basal lycosuchids and scylacosaurids was offset by increasing origination/extinction rates of eutherocephalians, which flourished into Wuchiapingian times. As a part of this radiation, whaitsioids represent a previously underappreciated but successful clade of late Permian eutherocephalians, but they did not survive the ecological impacts of the Permo-Triassic mass extinction. Future collecting will provide added resolution on the middle-to-late Permian transition, and will further clarify the dynamic replacement of basal therocephalians

687 (lycosuchids, scylacosaurids) by eutherocephalians and other early-diverging therapsid predators
688 (gorgonopsians, cynodonts).
689
690 ## ACKNOWLEDGMENTS
691
692 For collections access, we thank S. Kaal and the Iziko South African Museum, Cape
693 Town, and B. Rubidge and B. Zipfel of the Evolutionary Studies Institute (former Bernard Price
694 Institute, BP), Johannesburg. For comments on SAM-PK-K8516 and help in the field, we thank
695 S. Modesto. CT scans of SAM-PK-K8516 were produced by the University of Utah Core
696 Imaging Facility, Salt Lake City.
697
698 ## REFERENCES
699
700 Abdala, F. 2007. Redescription of *Platycraniellus elegans* (Therapsida, Cynodontia) from the
701 Lower Triassic of South Africa, and the cladistic relationships of eutheriodonts.
702 Palaeontology 50:591–618.
703 Abdala, F., T. Jashashvili, B. S. Rubidge, and J. van den Heever. 2014. New material of
704 *Microgomphodon oligocynus* (eutherapsida, therocephalia) and the taxonomy of southern
705 african bauriidae, p. 209–231 in C. F. Kammerer, K. D. Angielczyk, and J. Fröbisch
706 (eds.) Early Evolutionary History of the Synapsida. Springer, Dordrecht.
707 Abdala, F., C. F. Kammerer, M. O. Day, S. Jirah, and B. S. Rubidge. 2014. Adult morphology of
708 the therocephalian *Simorhinella baini* from the middle Permian of South Africa and the

taxonomy, paleobiogeography, and temporal distribution of the Lycosuchidae. Journal of Paleontology 88:1139–1153.

Abdala, F., B. S. Rubidge, and J. van den Heever. 2008. The oldest therocephalians (Therapsida, Eutheriodontia) and the early diversification of Therapsida. Palaeontology 51:1011–1024.

Attridge, J. 1956. The morphology and relationships of a complete therocephalian skeleton from the *Cistecephalus* Zone of South Africa. Proceedings of the Royal Society of Edinburgh. Section B 66:59–93.

Benton, M. J., A. J. Newell, G. D. Price, and A. A. Kurkin. 2012. Preservation of exceptional vertebrate assemblages in Middle Permian fluviolacustrine mudstones of Kotel'nich, Russia: stratigraphy, sedimentology, and taphonomy. Palaeogeography, Palaeoclimatology, Palaeoecology 319:58–83.

Botha, J., F. Abdala, and R. Smith. 2007. The oldest cynodont: new clues on the origin and early diversification of Cynodontia. Zoological Journal of the Linnean Society 149:477–492.

Botha-Brink, J., D. Codron, A. K. Huttenlocker, K. D. Angielczyk, and M. Ruta. 2016. Breeding young as a survival strategy during Earth's greatest mass extinction. Scientific Reports 6:24053.

Brink, A. S. 1956. On *Aneugomphius ictidoceps* Broom & Robinson. Palaeontologia Africana 4:97–115.

Brink, A. S. 1980. On the genus *Theriognathus* Owen (including *Whaitsia*, *Notosollasia*, *Alopecopsis*, *Notaelurops*, *Moschorhynchus* and *Aneugomphius*). Annals of the Geological Survey of South Africa 14:1–37.

Brocklehurst, N., M. Ruta, J. Müller, and J. Fröbisch. 2015. Elevated extinction rates as a trigger for diversification rate shifts: early amniotes as a case study. Scientific Reports 5:17104.

732 Broom, R. 1911. On some new South African Permian reptiles. Proceedings of the Zoological
733 Society of London 81:1073–1082.
734 Broom, R. 1935. On some new genera and species of Karroo fossil reptiles. Annals of the
735 Transvaal Museum 18:55–72.
736 Broom, R. 1948. A contribution to our knowledge of the vertebrates of the Karoo beds of South
737 Africa. Transactions of the Royal Society of Edinburgh 61:577–629.
738 Cole, D. I. 1992. Evolution and development of the Karoo Basin, Pp. 87-99 in M.J. De Wit &
739 I.G.D. Ransome (eds.), Inversion Tectonics of the Cape Fold Belt, Karoo and Cretaceous
740 Basins of Southern Africa, A.A. Balkema, Rotterdam.
741 Crompton, A. W. 1955. A revision of the scaloposauridae with special reference to kinetism in
742 this family. Navorsinge Van Die Nasionale Museum 1:149–183.
743 Day, M. O., S. Güven, F. Abdala, S. Jirah, B. Rubidge, and J. Almond. 2015a. Youngest
744 dinocephalian fossils extend the *Tapinocephalus* Zone, Karoo Basin, South Africa. South
745 African Journal of Science 111:1–5.
746 Day, M. O., J. Ramezani, S. A. Bowring, P. M. Sadler, D. H. Erwin, F. Abdala, and B. S.
747 Rubidge. 2015b. When and how did the terrestrial mid-Permian mass extinction occur?
748 Evidence from the tetrapod record of the Karoo Basin, South Africa. *Proc. R. Soc. B*
749 282(1811):20150834.
750 Fröbisch, J. 2008. Global taxonomic diversity of anomodonts (Tetrapoda, Therapsida) and the
751 terrestrial rock record across the Permian-Triassic boundary. PLoS One 3(11):e3733.
752 Fröbisch, J. 2013. Vertebrate diversity across the end-Permian mass extinction—Separating
753 biological and geological signals. Palaeogeography, Palaeoclimatology, Palaeoecology
754 372:50–61.

755 Golubev, V. K. 2000. The faunal assemblages of Permian terrestrial vertebrates from Eastern
756 Europe. Paleontological Journal 34(suppl. 2):S211–S224.
757 Haughton, S. H. 1918. Some new carnivorous Therapsida, with notes upon the braincase in
758 certain species. Annals of the South African Museum 12:175–216.
759 Heever, J. A. van den. 1994. The cranial anatomy of the early Therocephalia (Amniota:
760 Therapsida). Annals of the University of Stellenbosch 1:1–59.
761 Hillenius, W. J. 1994. Turbinates in therapsids: evidence for Late Permian origins of mammalian
762 endothermy. Evolution 48:207–229.
763 Hopson, J. A., and H. R. Barghusen. 1986. An analysis of therapsid relationships. Pp. 83–106 in
764 N. Hotton, P. D. MacLean, J. J. Roth, and E. C. Roth (eds.) The Ecology and Biology of
765 Mammal-like Reptiles. Smithsonian Institution Press, Washington.
766 Huttenlocker, A. K. 2009. An investigation into the cladistic relationships and monophyly of
767 therocephalian therapsids (Amniota: Synapsida). Zoological Journal of the Linnean
768 Society 157:865–891.
769 Huttenlocker, A. K. 2013. Paleobiology of therocephalian synapsids (Amniota) and the effects of
770 the end-Permian extinction on size, growth and bone microstructure. Ph.D. dissertation,
771 University of Washington, Seattle.
772 Huttenlocker, A. K. 2014. Body size reductions in nonmammalian eutheriodont therapsids
773 (Synapsida) during the end-Permian mass extinction. PLoS One 9:e87553.
774 Huttenlocker, A. K. and F. Abdala. 2015. Revision of the first therocephalian, *Theriognathus*
775 *microps* Owen (Therapsida: Whaitsiidae), and implications for cranial ontogeny and
776 allometry in nonmammalian eutheriodonts. Journal of Paleontology 89:645–664.

777 Huttenlocker, A. K., and J. Botha-Brink. 2013. Body size and growth patterns in the
778 therocephalian *Moschorhinus kitchingi* (Therapsida: Eutheriodontia) before and after the
779 end-Permian extinction in South Africa. Paleobiology 39:253–277.
780 Huttenlocker, A. K., and J. Botha-Brink. 2014. Bone microstructure and the evolution of growth
781 patterns in Permo-Triassic therocephalians (Amniota, Therapsida) of South Africa. PeerJ
782 2:e325.
783 Huttenlocker, A. K., and C. A. Sidor. 2012. Taxonomic revision of therocephalians (Therapsida:
784 Theriodontia) from the Lower Triassic of Antarctica. American Museum Novitates
785 3738:1–19.
786 Huttenlocker, A. K., and C. A. Sidor. 2016. The first karenitid (Therapsida, Therocephalia) from
787 the upper Permian of Gondwana and the biogeography of Permo-Triassic
788 therocephalians. Journal of Vertebrate Paleontology 36:e1111897.
789 Huttenlocker, A. K., C. A. Sidor, and K. D. Angielczyk. 2015. A new eutherocephalian
790 (Therapsida, Therocephalia) from the upper Permian Madumabisa Mudstone Formation
791 (Luangwa Basin) of Zambia. Journal of Vertebrate Paleontology 35:e969400.
792 Huttenlocker, A. K., C. A. Sidor, and R. M. H. Smith. 2011. A new specimen of
793 *Promoschorhynchus* (Therapsida: Therocephalia: Akidnognathidae) from the Lower
794 Triassic of South Africa and its implications for theriodont survivorship across the
795 Permo-Triassic boundary. Journal of Vertebrate Paleontology 31:405–421.
796 Irmis, R. B., J. H. Whiteside, and C. F. Kammerer. 2013. Non-biotic controls of observed
797 diversity in the paleontologic record: An example from the Permo-Triassic Karoo Basin
798 of South Africa. Palaeogeography, Palaeoclimatology, Palaeoecology 372:62–77.

799 Ivakhnenko, M. F. 2011. Permian and Triassic therocephals (Eutherapsida) of Eastern Europe.
800 Paleontological Journal 45:981–1144.
801 Kemp, T. S. 1972a. Whaitsiid Therocephalia and the origin of cynodonts. Philosophical
802 Transactions of the Royal Society of London: Series B 264:1-54.
803 Kemp, T.S. 1972b. The jaw articulation and musculature of the whaitsiid Therocephalia; pp.
804 213-230 in K.A. Joysey & T.S. Kemp (eds.), *Studies in Vertebrate Evolution.* Winchester
805 Press, New York, U.S.
806 Kemp, T. S. 2012. The origin and radiation of therapsids. pp. 2–28 in A. Chinsamy (ed.)
807 Forerunners of Mammals: Radiation, Histology, Biology. Indiana University Press,
808 Bloomington.
809 Lewis, P. O. 2001. A likelihood approach to estimating phylogeny from discrete morphological
810 character data. Systematic Biology 50:913–925.
811 Liu, J., and F. Abdala. 2017. Therocephalian (Therapsida) and chroniosuchian (Reptiliomorpha)
812 from the Permo-Triassic transitional Guodikeng Formation of the Dalongkou Section,
813 Jimsar, Xinjiang, China. Vertebrata PalAsiatica 55:24–40.
814 Lucas, S. G. 2017. Permian tetrapod extinction events. Earth-Science Reviews 170:31–60.
815 Mendrez, C. H. 1974a. Etude du crane d'un jeune specimen de *Moschorhinus kitchingi* Broom, 1920
816 (?*Tigrisuchus simus* Owen, 1876), Therocephalia, Pristerosauria, Moschorhinidae d'Afrique
817 Australe (Remarques sur les Moschorhinidae et les Whaitsiidae). Annals of the South
818 African Museum 64:71–115. [In French.]
819 Owen, R. 1876. Descriptive and Illustrated Catalogue of the Fossil Reptilia of South Africa in
820 the Collection of the British Museum. Printed by order of the Trustees, London.
821 Ronquist, F., P. van der Mark, and J. P. Huelsenbeck. 2009. Bayesian phylogenetic analysis

using MrBayes: Pp. 210–266 in A. M. Vandamme, M. Salemi, and P. Lemey (eds.) The Phylogenetic Handbook 2nd Edition. Cambridge University Press, Cambridge.

Rosset, A., L. Spadola, and O. Ratib. 2004. OsiriX: An open-source software for navigating in multidimensional DICOM images. J. Digit. Imaging 17.

Rubidge, B. S., D. H. Erwin, J. Ramezani, S. A. Bowring, and W. J. de Klerk. 2013. High-precision temporal calibration of late Permian vertebrate biostratigraphy: U-Pb zircon constraints from the Karoo Supergroup, South Africa. Geology 41:363–366.

Sidor, C.A., D. A. Vilhena, K. D. Angielczyk, A. K. Huttenlocker, S. J. Nesbitt, B. R. Peecook, J. S. Steyer, R. M. H. Smith and L. A. Tsuji. 2013. Provincialization of terrestrial faunas following the end-Permian mass extinction. Proceedings of the National Academy of Sciences 110:8129–8133.

Sigurdsen, T. 2006. New features of the snout and orbit of a therocephalian therapsid from South Africa. Acta Palaeontologica Polonica 51:63–75.

Sigurdsen, T., A. K. Huttenlocker, S. P. Modesto, T. B. Rowe, and R. Damiani. 2012. Reassessment of the morphology and paleobiology of the therocephalian *Tetracynodon darti* (Therapsida), and the phylogenetic relationships of Baurioidea. Journal of Vertebrate Paleontology 32:1113–1134.

Smith, R. M. H. 1987. Morphology and depositional history of exhumed Permian point bars in the southwestern Karoo, South Africa. Journal Sedimentary Petrology 57:19-29.

Smith, R. M. H. 1990. Alluvial paleosols and pedofacies sequences in the Permian Lower Beaufort of the southwestern Karoo Basin, South Africa. Journal Sedimentary Petrology 60:258-276

844 Smith, R. M. H. 1993. Vertebrate taphonomy of Late Permian floodplain deposits in the
845 southwestern Karoo Basin of South Africa. Palaios 8:45–67.
846 Smith, R.M. H., and J. Botha-Brink. 2011. Morphology and composition of bone-bearing
847 coprolites from the Late Permian Beaufort Group, Karoo Basin, South Africa.
848 Palaeogeography, Palaeoclimatology, Palaeoecology 312:40–53.
849 Smith, R. M. H., B. Rubidge, and M. van der Walt. 2012. Therapsid biodiversity patterns and
850 paleoenvironments of the Karoo Basin, South Africa: pp. 30–62 in A. Chinsamy (ed.)
851 Forerunners of Mammals: Radiation, Histology, Biology. Indiana University Press,
852 Bloomington.
853 Swofford, D. 1999. PAUP* Phylogenetic analysis using parsimony v. 4.0 beta 10. Sinauer
854 Associates, Sunderland, MA.
855 Tatarinov, L. P. 1963. A new Late Permian therocephalian. Paleontological Journal 4:76–94.
856 Tatarinov, L. P. 1974. Theriodonts of the USSR. Trudy Paleontologicheskogo Instituta,
857 Akademii Nauk SSSR 143:1–240. [in Russian]
858 Tatarinov, L. P. 1995. *Viatkosuchus sumini*, a new Late Permian therocephalian from the Kirov
859 region. Paleontological Journal 29:111–128.
860 Turner, B. R. 1978. Sedimentary patterns of uranium mineralization in the Beaufort Group of the
861 southern Karoo (Gondwana) Basin, South Africa. In: A.D.Miall (Editor), Fluvial
862 Sedimentology, Canadian Association of Petroleum Geologists. Memoir 5:831–848.
863 Watson, D. M. S., and A. S. Romer. 1956. A classification of therapsid reptiles. Bulletin of the
864 Museum of Comparative Zoology, Harvard 111:37–89.
865
866

867

868

869

870

871
872
873 FIGURE & TABLE LEGENDS

874

875 FIGURE 1. Specimen provenance and stratigraphic context of Teekloof Formation whaitsioids.
876 1, Provenance of SAM-PK-K10990 and K10984, Badshoek farm (De Hoop 117), near Beaufort
877 West, Western Cape Province; 2, Provenance of SAM-PK- K8516, Good Luck farm, near
878 Fraserburg, Northern Cape Province. Bulleted numbers to right of stratigraphic column indicate
879 ages of vertebrate assemblage zones in millions of years (**Ma**) (from Rubidge et al., 2013).
880 Geologic map modified from Smith (1993). **Abbreviations**: ***Ci*AZ**, *Cistecephalus* Assemblage
881 Zone; ***Dapto*AZ**, *Daptocephalus* Assemblage Zone; **Fm**, Formation; **M**, Member; ***Prist*AZ**,
882 *Pristerognathus* Assemblage Zone; ***Tapino*AZ**, *Tapinocephalus* Assemblage Zone; ***Tr*AZ**,
883 *Tropidostoma* Assemblage Zone. [full page width]

884

885 FIGURE 2. Holotypic skull of *Microwhaitsia mendrezi* gen. et sp. nov. (SAM-PK-K10990) in
886 dorsal (**A**), ventral (**B**), and right lateral (**C**) views. [full page width]

887

888 FIGURE 3. Interpretive line drawings of the holotypic skull of *Microwhaitsia mendrezi* gen. et
889 sp. nov. (SAM-PK-K10990) in dorsal (**A**), ventral (**B**), and right lateral (**C**) views.
890 **Abbreviations**: **d**, dentary; **C**, upper canine; **cr.ch**, crista choanalis; **f**, frontal; **f.l**, lacrimal

foramen; **I5**, fifth upper incisor; **j**, jugal; **l**, lacrimal; **m**, maxilla; **n**, nasal; **p**, parietal; **pal**, palatine; **pC**, upper precanine; **PC5**, fifth upper postcanine; **po**, postorbital; **pm**, premaxilla; **prf**, prefrontal; **pt**, pterygoid; **sa**, surangular; **sm**, septomaxilla; **sp**, splenial. [full page width]

FIGURE 4. Stereopair images of the palate of the holotypic skull of *Microwhaitsia mendrezi* gen. et sp. nov. (SAM-PK-K10990) in left oblique ventral (**A**) and posteroventral (**B**) views. Note the narrow contact between the left crista choanalis and vomer without sutural connection. [two-thirds page width]

FIGURE 5. Referred specimen of *Microwhaitsia mendrezi* gen. et sp. nov. (SAM-PK-K10984) in dorsal (**A**), ventral (**B**), and left lateral (**C**) views. [one column's width]

FIGURE 6. Interpretive line drawings of referred specimen of *Microwhaitsia mendrezi* gen. et sp. nov. (SAM-PK-K10984) in dorsal (**A**), ventral (**B**), and left lateral (**C**) views. **Abbreviations**: **C**, upper canine alveolus; **cr.ch**, crista choanalis; **ect**, ectopterygoid; **f**, frontal; **j**, jugal; **l**, lacrimal; **m**, maxilla; **m.pal.f**, maxillo-palatine foramen; **n**, nasal; **pal**, palatine; **PC5**, fifth upper postcanine alveolus; **prf**, prefrontal; **pt**, pterygoid; **v**, vomer; **v.suborb**, suborbital vacuity. [one column's width]

FIGURE 7. Volumized HRXCT scans of the skull of *Ophidostoma tatarinovi* gen. et sp. nov. (SAM-PK-K8516) in dorsal (**A**), ventral (**B**), left lateral (**C**), and frontal (**D**) views. [full page width]

914 FIGURE 8. Interpretive line drawings of the skull of *Ophidostoma tatarinovi* gen. et sp. nov.
915 (SAM-PK-K8516) in dorsal (**A**), ventral (**B**), left lateral (**C**), and frontal (**D**) views.
916 **Abbreviations**: **a**, angular; **d**, dentary; **ect**, ectopterygoid; **c**, lower canine; **C**, upper canine; **f**,
917 frontal; **fen.m**, mandibular fenestra; **i**, lower incisor; **j**, jugal; **l**, lacrimal; **m**, maxilla; **n**, nasal; **p**,
918 parietal; **part**, prearticular; **pbs**, para-basisphenoid; **PC6**, sixth upper postcanine; **po**, postorbital;
919 **pm**, premaxilla; **prf**, prefrontal; **pt**, pterygoid; **q-qj**, quadrate-quadratojugal complex; **sa**,
920 surangular; **sm**, septomaxilla; **sp**, splenial; **sq**, squamosal; **v.ipt**, interpterygoid vacuity;
921 **v.suborb**, suborbital vacuity. [full page width]
922
923 FIGURE 9. Major clades of eutherocephalians (tree length = 381; consistency index (CI) =
924 0.438; retention index = 0.789; rescaled CI = 0.346).
925
926 FIGURE 10. New specimen of the hofmeyriid *Mirotenthes digitipes* Attridge, 1956 (SAM-PK-
927 K11188) from the upper *Cistecephalus* Assemblage Zone of 'Good Luck.' Specimen shown in
928 dorsal oblique view, showing the large temporal fenestra and broad, anvil-shaped epipterygoid
929 (**ept**) processus ascendens. [two-thirds page width]
930
931 FIGURE 11. Stratigraphically calibrated phylogeny of middle Permian through Triassic
932 therocephalians showing calibration points for minimum divergence dates of major clades. Light
933 gray lines represent hypothetical phylogenetic branching, whereas black bars represent observed
934 stratigraphic ranges (dashed ends indicate taxa having unknown upper or lower ranges). Graph
935 (below) shows peak levels of eutherocephalian origination/extinction by the Wuchiapingian
936 stage. **Abbreviations**: **An**, Antarctica; **Ch**, China; **Chx**, Changxingian; ***Ci*AZ**, *Cistecephalus*

Assemblage Zone; ***Dapto*AZ**, *Daptocephalus* Assemblage Zone; **Ind**, Induan; **Na**, Namibia; **Olen**, Olenekian; ***Prist*AZ**, *Pristerognathus* Assemblage Zone; **Roa**, Roadian; **Ru**, Russia; **SA**, South Africa; ***Tapino*AZ**, *Tapinocephalus* Assemblage Zone; ***Tr*AZ**, *Tropidostoma* Assemblage Zone; **Tz**, Tanzania; **Wor**, Wordian; **Za**, Zambia. [full page]

FIGURE 12. Representative hofmeyriid from the late Capitanian or earliest Wuchiapingian of the Karoo Basin, South Africa, compared to other known specimens of *Hofmeyria*. SAM-PK-K10525 (**A**), Hofmeyriidae from the *Pristerognathus* Assemblage Zone of Lombardskraal, Beaufort West district, Western Cape Province. Specimen shows short, high rostrum, prefrontal-postorbital contact in orbit, anteriorly expanded epipterygoid, and conical, non-serrated/non-carinated maxillary teeth. BP/1/4404 (BP, former Bernard Price Institute, now Evolutionary Studies Institute, Johannesburg) (**B**), *Hofmeyria* cf. *H. atavus* from the *Cistecephalus* Assemblage Zone of Matjiesfontein (Highlands), Victoria West district, Northern Cape Province. BP/1/1399 (**C**), *Hofmeyria* cf. *H. atavus* from the *Cistecephalus* Assemblage Zone of Driehoeksfontein, Murraysburg district, Western Cape Province. Numbers 14–136 are characters listed in the phylogenetic analysis (see online Supplemental Appendix) followed by the derived state in parentheses corresponding to hofmeyriids or other early whaitsioids. **Abbreviations**: **AZ**, Assemblage Zone; **PC**, postcanine position #. [full page]

TABLE 1. List of tetrapod fossils collected from the two farms ‘Badshoek’ and ‘Good Luck’ by the Iziko South African Museum between 1996 and 2015. The newly described therocephalian species are bold.

960 TABLE 2. African Permo-Triassic therocephalians by Karoo assemblage zone or equivalent

961 (updated from Abdala et al., 2008 and Huttenlocker, 2013).

962

963 TABLE 3. Russian and Chinese Permo-Triassic therocephalians by assemblage zone or stage

964 (updated from Abdala et al., 2008, Ivakhnekno, 2011, and Huttenlocker, 2013).

965

966

Table 1(on next page)

Table 1

List of tetrapod fossils collected from the two farms ‘Badshoek’ and ‘Good Luck’ by the Iziko South African Museum between 1996 and 2015. The newly described therocephalian species are bold.

Table 1. List of tetrapod fossils collected from the two farms 'Badshoek' and 'Good Luck' by the Iziko South African Museum between 1996 and 2015. The newly described therocephalian species are bold.

Specimen Number	Identification	Stratigraphic Level
Good Luck (Matjiesfontein 412)		
SAM-PK-K11279	*Dicynodon* sp.	Steenkamp member (lower *Dapto*AZ)
SAM-PK-K11189	*Cistecephalus microrhinus*	Oukloof/Steenkamp (uppermost *Ci*AZ)
SAM-PK-K11188	*Mirotenthes digitipes*	Oukloof/Steenkamp (uppermost *Ci*AZ)
SAM-PK-K8630	*Pareiasaurus* sp.	Oukloof member (upper *Ci*AZ)
SAM-PK-K8508	*Diictodon* sp.	Oukloof member (upper *Ci*AZ)
SAM-PK-K8509	*Diictodon* sp.	Oukloof member (upper *Ci*AZ)
SAM-PK-K8513	*Diictodon* sp.	Oukloof member (upper *Ci*AZ)
SAM-PK-K8303	*Cistecephalus* sp.	Oukloof member (upper *Ci*AZ)
SAM-PK-K8304	*Cistecephalus* sp.	Oukloof member (upper *Ci*AZ)
SAM-PK-K8510	*Cistecephalus* sp.	Oukloof member (upper *Ci*AZ)
SAM-PK-K8512	*Cistecephalus* sp.	Oukloof member (upper *Ci*AZ)
SAM-PK-K8629	*Cistecephalus* sp.	Oukloof member (upper *Ci*AZ)
SAM-PK-K11187	*Cistecephalus* sp.	Oukloof member (upper *Ci*AZ)
SAM-PK-K8307	*Oudenodon* sp.	Oukloof member (upper *Ci*AZ)
SAM-PK-K11280	*Oudenodon* sp.	Oukloof member (upper *Ci*AZ)
SAM-PK-K8507	*Dicynodon* sp.	Oukloof member (upper *Ci*AZ)
SAM-PK-K8516	***Ophidostoma tatarinovi*** (type)	Oukloof member (upper *Ci*AZ)
SAM-PK-K8631	Eutherocephalia indet.	Oukloof member (upper *Ci*AZ)
SAM-PK-K8511	*Procynosuchus delaharpeae*	Oukloof member (upper *Ci*AZ)
SAM-PK-K11186	*Procynosuchus delaharpeae*	Oukloof member (upper *Ci*AZ)
Badshoek (De Hoop 117)		
SAM-PK-K10449	*Pristerodon* sp.	Oukloof member (*Ci*AZ)
SAM-PK-K11008	*Pristerodon* sp.	Hoedemaker member (upper *Tr*AZ)
SAM-PK-K11009	*Pristerodon* sp.	Hoedemaker member (upper *Tr*AZ)
SAM-PK-K11010	*Pristerodon* sp.	Hoedemaker member (upper *Tr*AZ)
SAM-PK-K11011	*Diictodon* sp.	Hoedemaker member (upper *Tr*AZ)
SAM-PK-K10987	*Pristerodon* sp.	Hoedemaker member (*Tr*AZ)
SAM-PK-K10985	*Diictodon* sp.	Hoedemaker member (*Tr*AZ)
SAM-PK-K10986	*Emydops* sp.	Hoedemaker member (*Tr*AZ)
SAM-PK-K11000	*Tropidostoma* sp.	Hoedemaker member (*Tr*AZ)
SAM-PK-K10983	Gorgonopsia indet.	Hoedemaker member (*Tr*AZ)
SAM-PK-K10984	***Microwhaitsia mendrezi***	Hoedemaker member (*Tr*AZ)
SAM-PK-K10990	***Microwhaitsia mendrezi*** (type)	Hoedemaker member (*Tr*AZ)

*Ci*AZ, *Cistecephalus* Assemblage Zone; *Dapto*AZ, *Daptocephalus* Assemblage Zone; *Tr*AZ, *Tropidostoma* Assemblage Zone.

Table 2(on next page)

Table 2

African Permo-Triassic therocephalians by Karoo assemblage zone or equivalent (updated from Abdala et al., 2008 and Huttenlocker, 2013).

Table 2. African Permo-Triassic therocephalians by Karoo assemblage zone or equivalent (updated from Abdala et al., 2008 and Huttenlocker, 2013).

Permian

Eodicynodon Assemblage Zone (Wordian) (2)
- *Glanosuchus macrops*
- *Ictidosaurus angusticeps*

Tapinocephalus Assemblage Zone (Capitanian) (8)
- *Alopecodon priscus*
- *Blattoidealestes gracilis**
- *Crapartinella croucheri**
- *Glanosuchus macrops*
- *Ictidosaurus angusticeps*
- *Lycosuchus vanderrieti*
- *Pardosuchus whaitsi*
- *Pristerognathus polyodon*
- *Scylacosaurus sclateri*
- *Simorhinella baini*

Pristerognathus Assemblage Zone (late Capitanian–Wuchiapingian) (5)
- *Glanosuchus macrops*
- Hofmeyriidae (cf. *Hofmeyria*)
- Ictidosuchidae (cf. *Ictidosuchoides*)
- *Lycosuchus vanderrieti*
- *Pristerognathus polyodon*

Tropidostoma Assemblage Zone (Wuchiapingian) (6)
- *Choerosaurus dejageri*
- *Hofmeyria atavus*
- *Ictidostoma hemburyi*
- *Ictidosuchoides longiceps*
- *Ictidosuchus primaevus*
- *Microwhaitsia mendrezi*

Cistecephalus Assemblage Zone (Wuchiapingian) (8)
- *Mupashi migrator*
- *Euchambersia mirabilis*
- *Hofmeyria atavus*
- *Ichibengops munyamadziensis*
- *Ictidostoma hemburyi*
- *Ictidosuchoides longiceps*
- *Mirotenthes digitipes*
- *Ophidostoma tatarinovi*
- *Polycynodon elegans*
- *Theriognathus microps*
- Unnamed akidnognathid (USNM PAL 412421)

Daptocephalus Assemblage Zone (Wuchiapingian–Changxingian) (11)
- *Akidnognathus parvus*
- *Cerdosuchoides brevidens*
- *Ictidochampsa platyceps*
- *Ictidosuchoides longiceps*
- *Ictidosuchops rubidgei*
- *Lycideops longiceps*

Mirotenthes digitipes
Moschorhinus kitchingi
Promoschorhynchus platyrhinus
Tetracynodon tenuis
Theriognathus microps

Triassic
Lystrosaurus Assemblage Zone (Induan–Olenekian) (7)
Ericiolacerta parva
Moschorhinus kitchingi
Olivierosuchus parringtoni
Promoschorhynchus cf. *P. platyrhinus* †
Regisaurus jacobi
Scaloposaurus constrictus
Tetracynodon darti
Cynognathus Assemblage Zone (Olenekian–Anisian) (2)
Bauria cynops
Microgomphodon oligocynus

* Taxa denoted by asterisk are considered invalid or based on non-diagnostic juvenile material;
†SAM-PK-K10014, originally identified as *Ictidosuchoides* (Smith and Botha, 2005; Botha and Smith, 2006; Abdala et al., 2008; Huttenlocker et al., 2011)

Table 3(on next page)

Table 3

Russian and Chinese Permo-Triassic therocephalians by assemblage zone or stage (updated from Abdala et al., 2008, Ivakhnekno, 2011, and Huttenlocker, 2013).

Table 3. Russian and Chinese Permo-Triassic therocephalians by assemblage zone or stage (updated from Abdala et al., 2008, Ivakhnekno, 2011, and Huttenlocker, 2013).

Permian

Wordian–Capitanian (*Ulemosaurus* Assemblage Zone, Isheevo fauna or equivalent) (2)
- *Perplexisaurus*(?) *lepusculus**
- *Porosteognathus efremovi*

late Capitanian–Wuchiapingian? (*Deltavjatia* Assemblage Zone, Kotelnich fauna or equivalent) (6)
- *Karenites ornamentatus*
- *Kotelcephalon viatkensis*
- *Perplexisaurus* (=*Chlynovia*) *foveatus*
- *Scalopodon tenuisfrons*
- *Scalopodontes kotelnichi*
- *Viatkosuchus sumini*

Wuchiapingian (*Proelginia* Assemblage Zone, Ilynskoe fauna or equivalent) (1)
- *Scylacosuchus orenburgensis*

Wuchiapingian-Changxingian? (*Scutosaurus* Assemblage Zone, Sokolki fauna or equivalent) (2)
- *Annatherapsidus petri*
- *Chthonosaurus velocidens*

Changxingian (*Archosaurus* Assemblage Zone, Vyazniki fauna or equivalent) (6)
- *Dalongkoua fuae*†
- *Hexacynodon purlinensis**
- *Malasaurus germanus**
- *Moschowhaitsia vjuschkovi*
- *Purlovia maxima*
- Whaitsiidae indet.

Triassic

Induan–Olenekian (Vetlugian stage or equivalent) (5)
- *Hazhenia concava*
- *Scalopognathus multituberculatus**
- *Silphedosuchus orenburgensis*
- *Urumchia lii*
- *Yikezhaogia megafenestrala*

Anisian (*Eryosuchus* Assemblage Zone, Donguzian fauna or equivalent) (7)
- *Antecosuchus ochevi*
- *Dongusaurus schepetovi*†
- *Nothogomphodon danilovi*
- *Nothogomphodon sanjiaoensis*
- *Ordosiodon lincheyuensis*
- *Ordosiodon youngi*
- *Traversodontoides wangwuensis*

* Taxa denoted by asterisk are considered invalid or based on non-diagnostic material

† Precise age uncertain. Regarded as Permo-Triassic by Liu and Abdala, 2017.

Figure 1

Specimen provenance and stratigraphic context of Teekloof Formation whaitsioids.

1, Provenance of SAM-PK-K10990 and K10984, Badshoek farm (De Hoop 117), near Beaufort West, Western Cape Province; 2, Provenance of SAM-PK- K8516, Good Luck farm, near Fraserburg, Northern Cape Province. Bulleted numbers to right of stratigraphic column indicate ages of vertebrate assemblage zones in millions of years (**Ma**) (from Rubidge et al., 2013). Geologic map modified from Smith (1993). **Abbreviations**: ***Ci*AZ**, *Cistecephalus* Assemblage Zone; ***Dapto*AZ**, *Daptocephalus* Assemblage Zone; **Fm**, Formation; **M**, Member; ***Prist*AZ**, *Pristerognathus* Assemblage Zone; ***Tapino*AZ**, *Tapinocephalus* Assemblage Zone; ***Tr*AZ**, *Tropidostoma* Assemblage Zone.

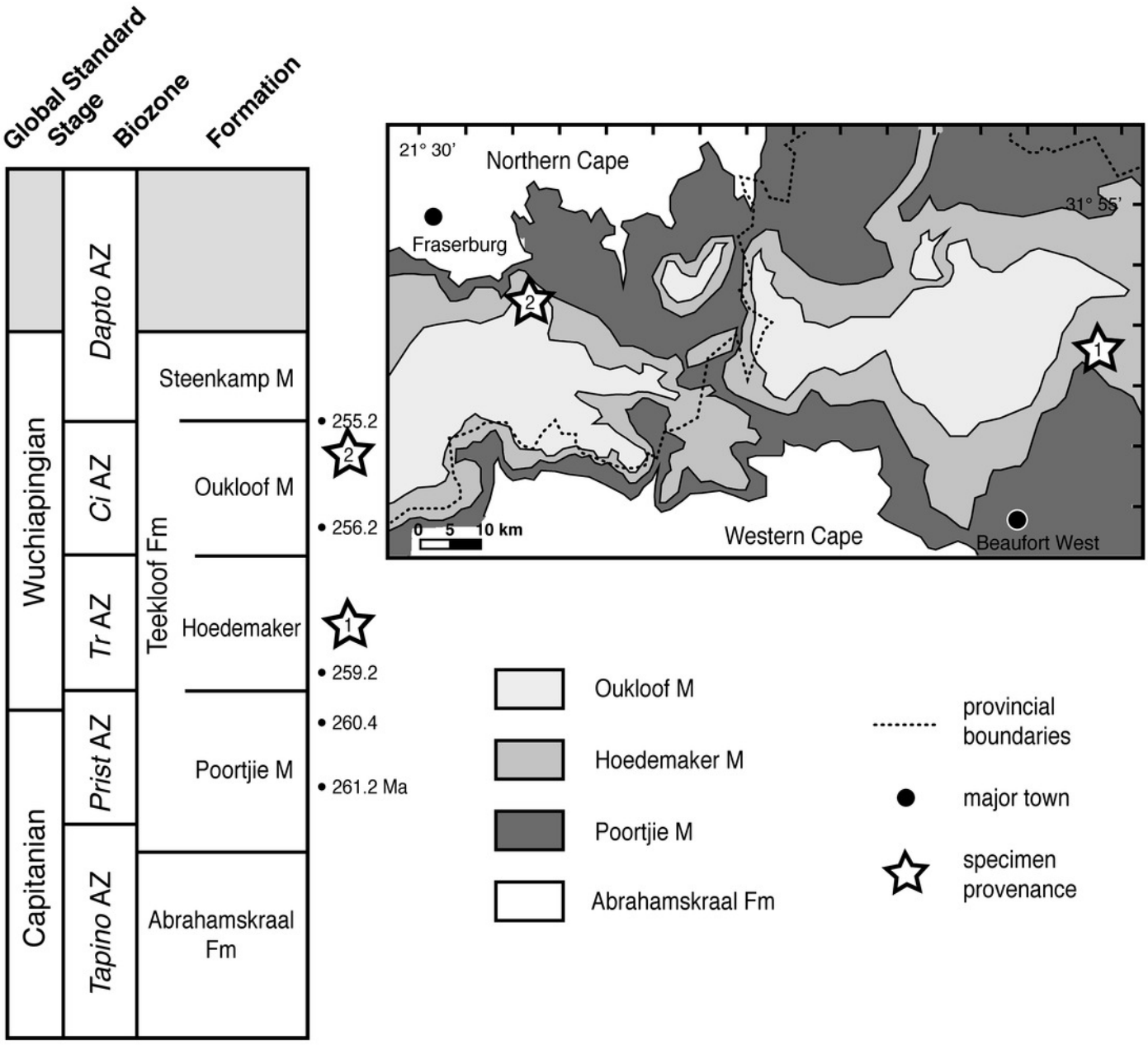
Global Standard Stage
Biozone
Formation
Wuchiapingian
Capitanian
Dapto AZ
Ci AZ
Tr AZ
Prist AZ
Tapino AZ
Teekloof Fm
Steenkamp M
Oukloof M
Hoedemaker
Poortjie M
Abrahamskraal Fm
255.2
256.2
259.2
260.4
261.2 Ma
21° 30'
Northern Cape
31° 55'
Fraserburg
Western Cape
Beaufort West
0 5 10 km
Oukloof M
Hoedemaker M
Poortjie M
Abrahamskraal Fm
provincial boundaries
major town
specimen provenance

Figure 2

Holotypic skull of *Microwhaitsia mendrezi* gen. et sp. nov. (SAM-PK-K10990) in dorsal (A), ventral (B), and right lateral (C) views.

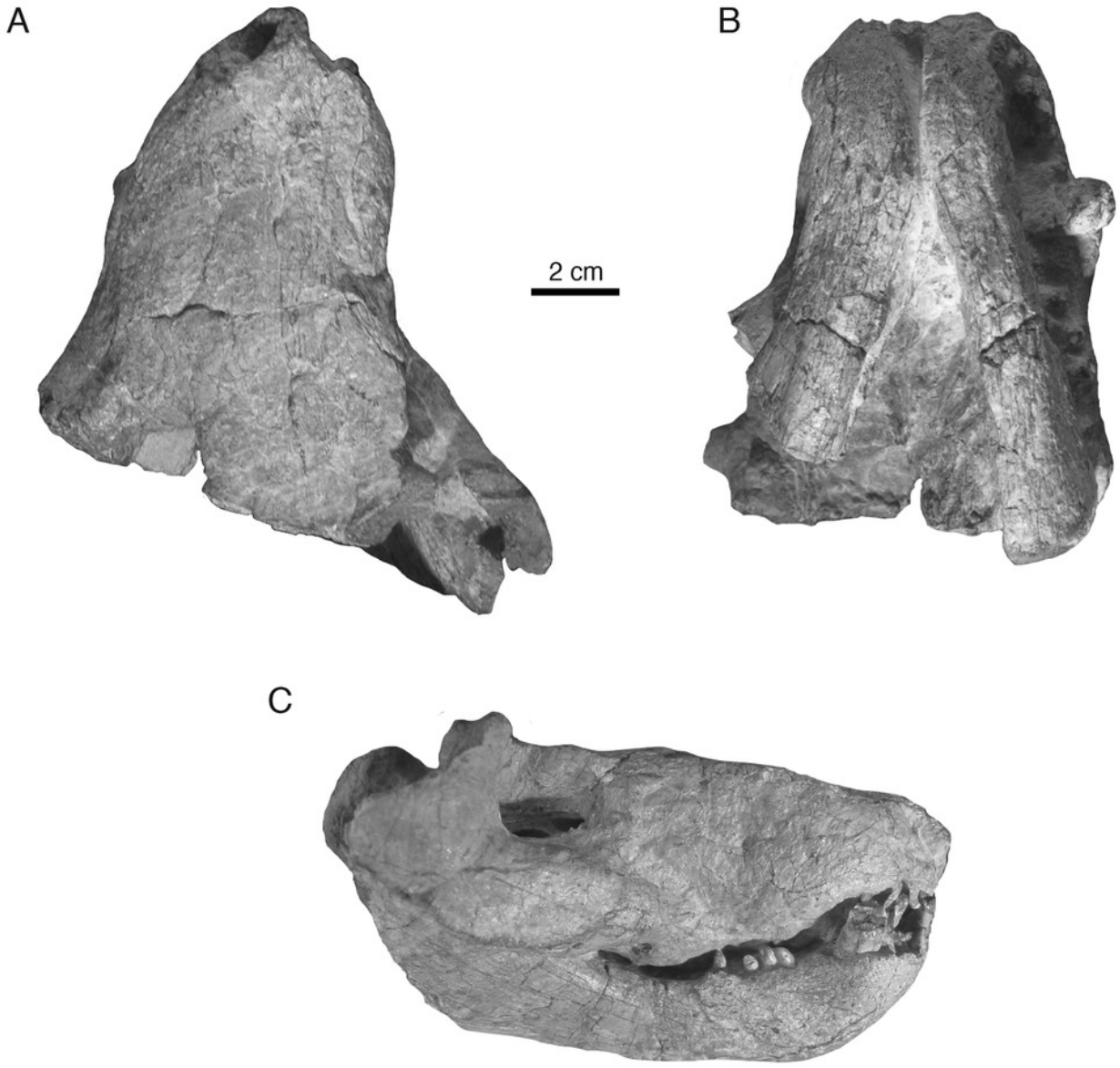

Figure 3

Interpretive line drawings of the holotypic skull of *Microwhaitsia mendrezi* gen. et sp. nov. (SAM-PK-K10990) in dorsal (A), ventral (B), and right lateral (C) views.

Abbreviations: **d**, dentary; **C**, upper canine; **cr.ch**, crista choanalis; **f**, frontal; **f.l**, lacrimal foramen; **I5**, fifth upper incisor; **j**, jugal; **l**, lacrimal; **m**, maxilla; **n**, nasal; **p**, parietal; **pal**, palatine; **pC**, upper precanine; **PC5**, fifth upper postcanine; **po**, postorbital; **pm**, premaxilla; **prf**, prefrontal; **pt**, pterygoid; **sa**, surangular; **sm**, septomaxilla; **sp**, splenial.

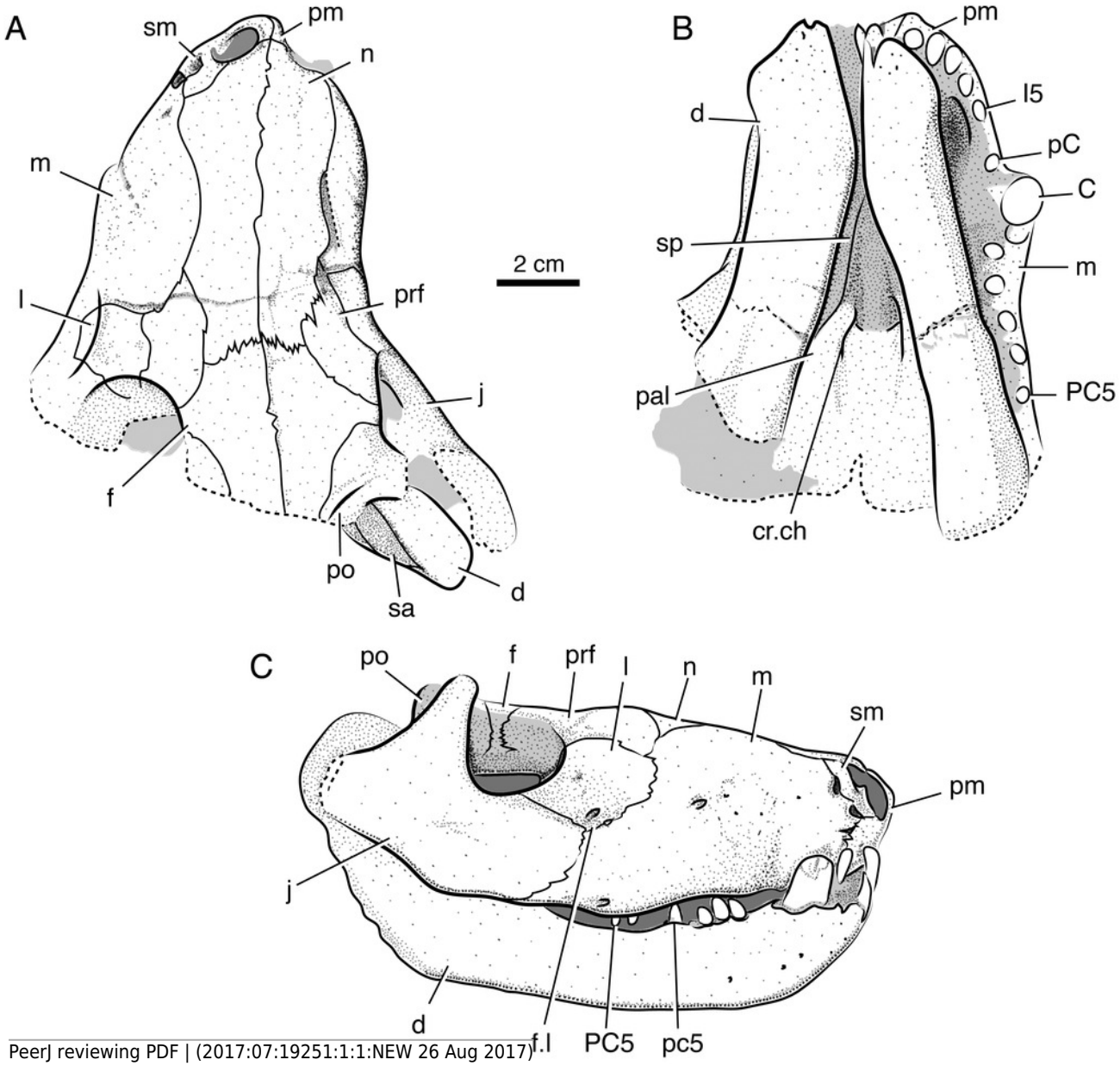

Figure 4

Stereopair images of the palate of the holotypic skull of *Microwhaitsia mendrezi* gen. et sp. nov. (SAM-PK-K10990) in left oblique ventral (A) and posteroventral (B) views.

Note the narrow contact between the left crista choanalis and vomer without sutural connection

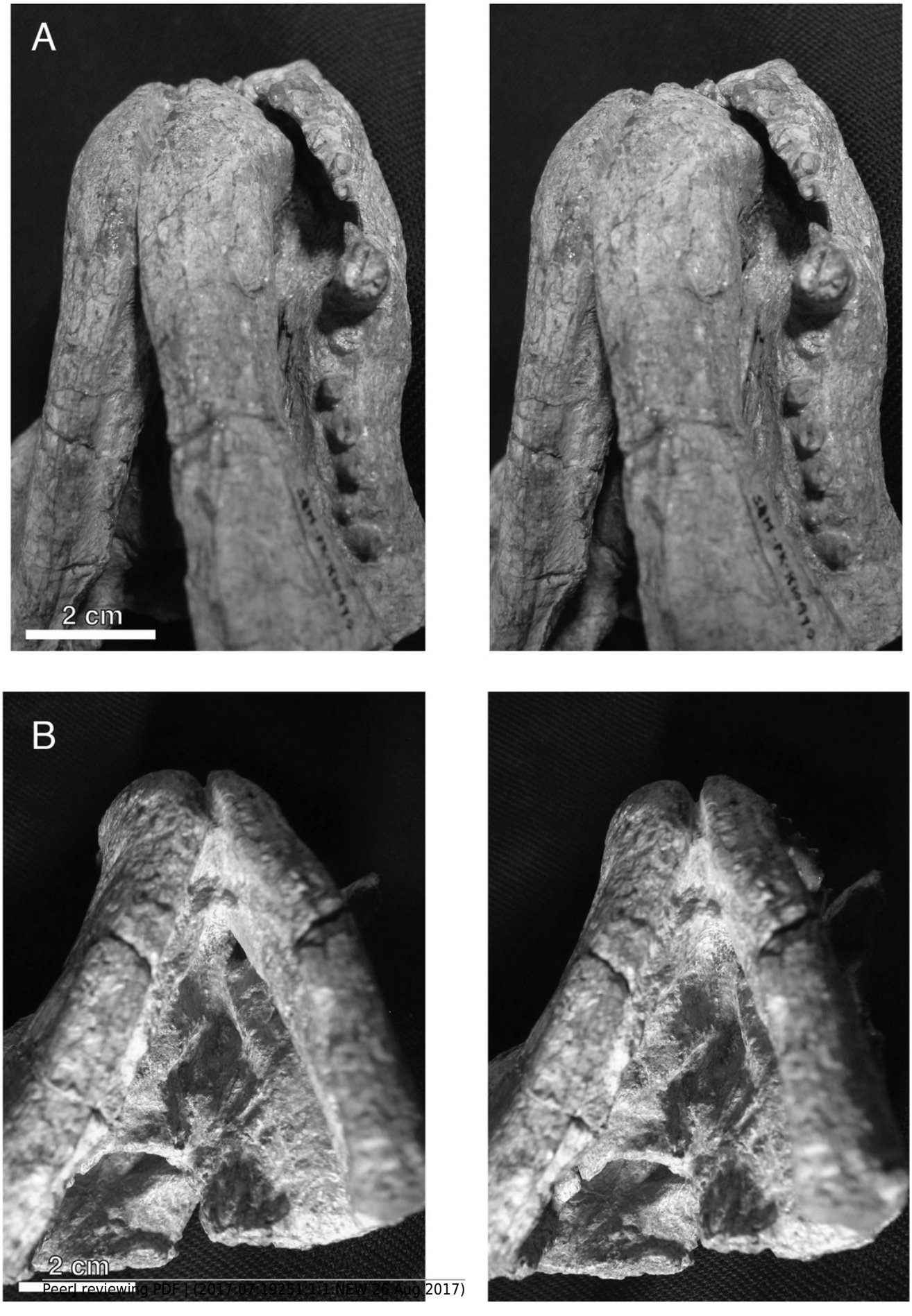
A
2 cm
B
2 cm

Figure 5

Referred specimen of *Microwhaitsia mendrezi* gen. et sp. nov. (SAM-PK-K10984) in dorsal (A), ventral (B), and left lateral (C) views.

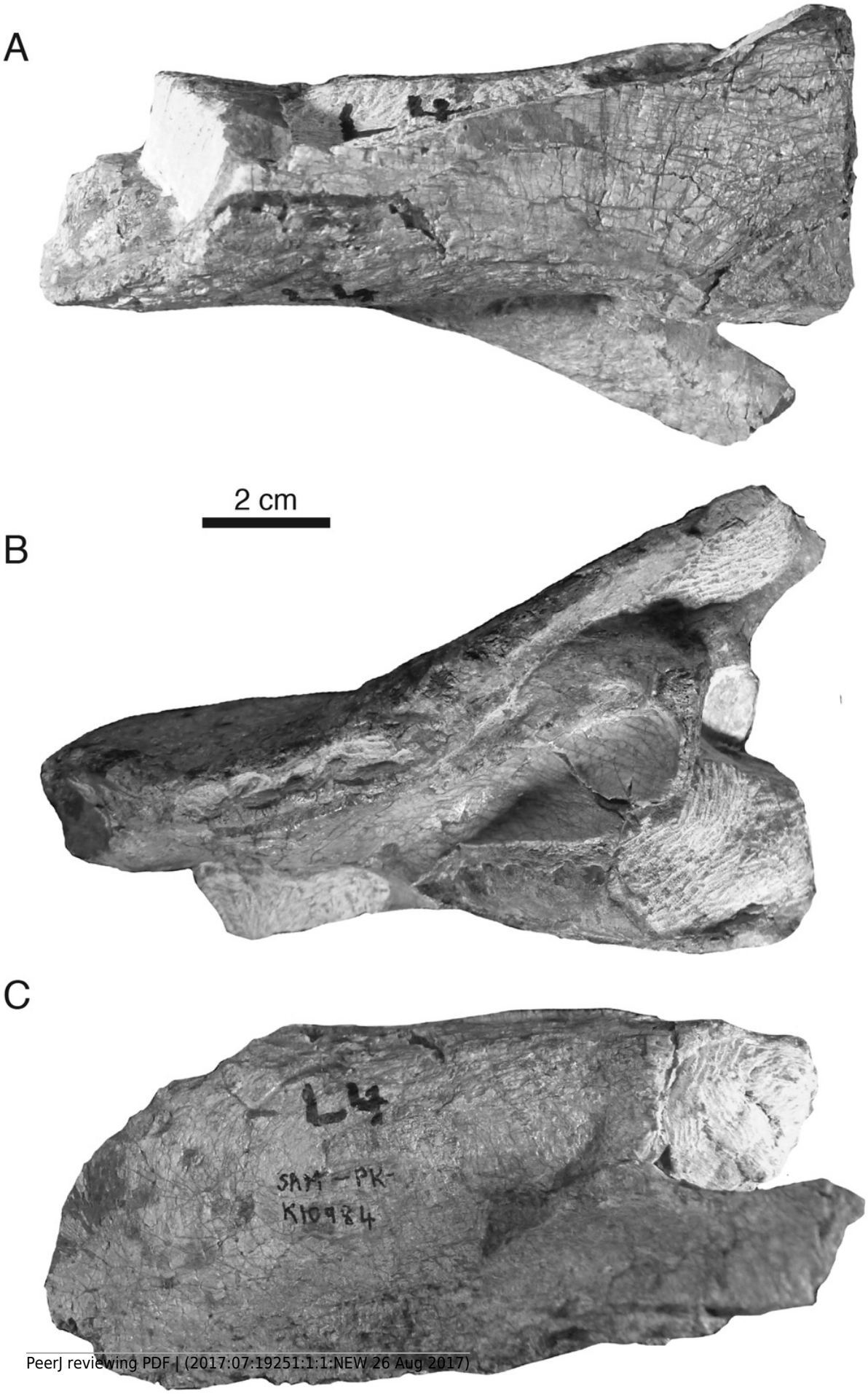
A
2 cm
B
C
L4
SAM-PK-
K10984

Figure 6

Interpretive line drawings of referred specimen of *Microwhaitsia mendrezi* gen. et sp. nov. (SAM-PK-K10984) in dorsal (A), ventral (B), and left lateral (C) views.

Abbreviations: **C**, upper canine alveolus; **cr.ch**, crista choanalis; **ect**, ectopterygoid; **f**, frontal; **j**, jugal; **l**, lacrimal; **m**, maxilla; **m.pal.f**, maxillo-palatine foramen; **n**, nasal; **pal**, palatine; **PC5**, fifth upper postcanine alveolus; **prf**, prefrontal; **pt**, pterygoid; **v**, vomer; **v.suborb**, suborbital vacuity.

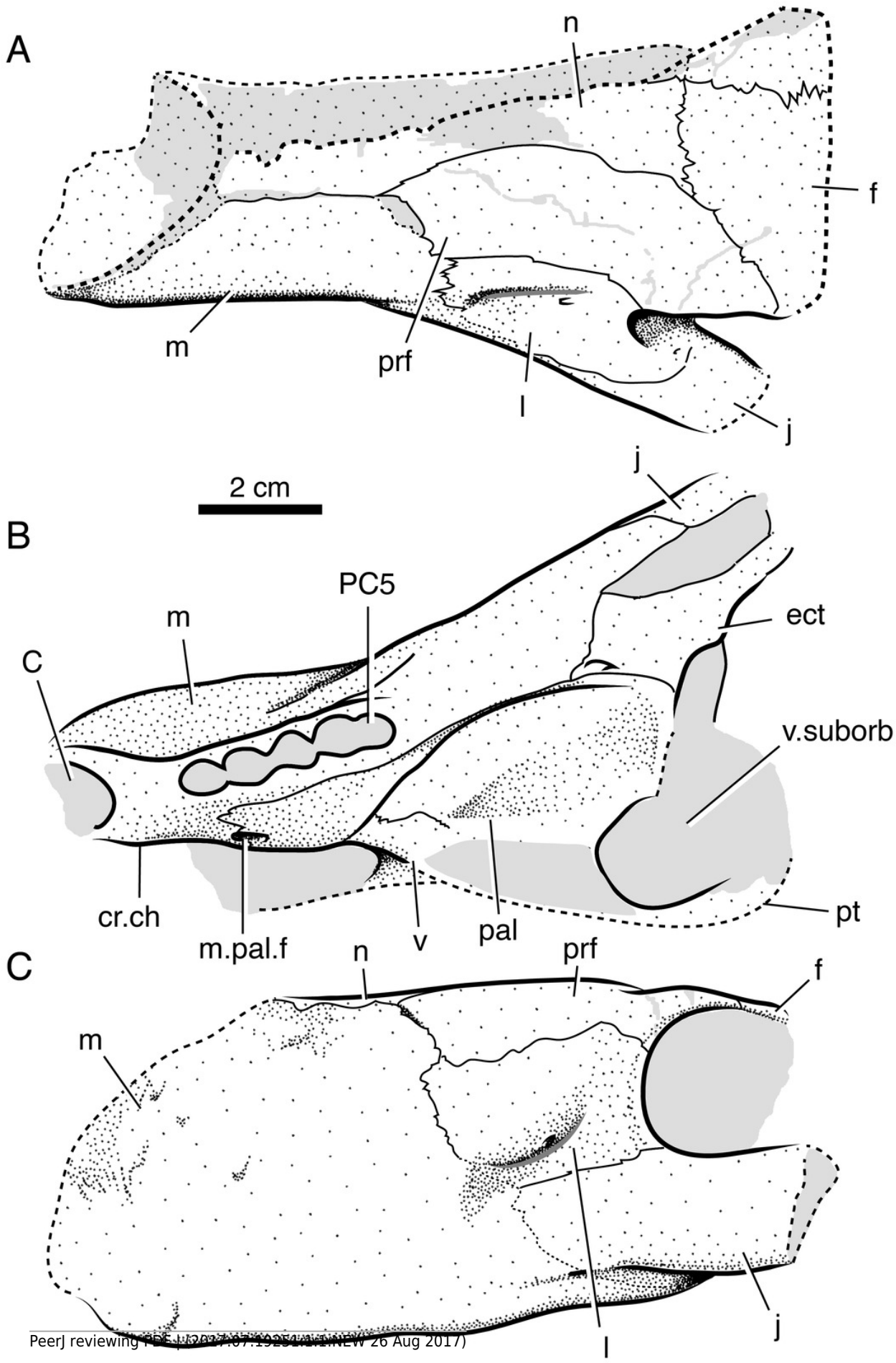
A
n
f
m
prf
l
j
2 cm
B
j
PC5
m
ect
C
v.suborb
cr.ch
m.pal.f
v
pal
pt
C
n
prf
f
m
j
l

Figure 7

Volumized HRXCT scans of the skull of *Ophidostoma tatarinovi* gen. et sp. nov. (SAM-PK-K8516) in dorsal (A), ventral (B), left lateral (C), and frontal (D) views.

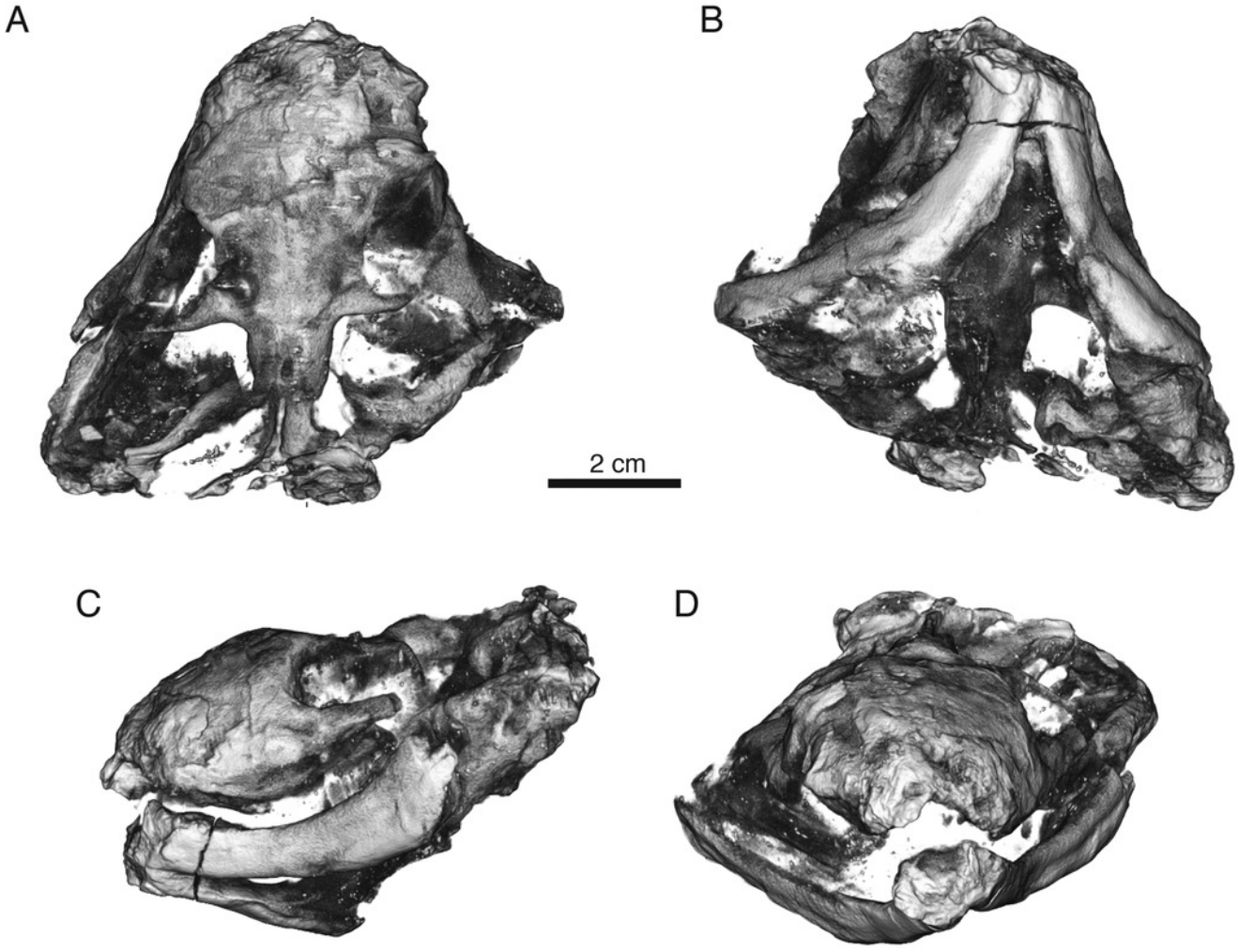

Figure 8

Interpretive line drawings of the skull of *Ophidostoma tatarinovi* gen. et sp. nov. (SAM-PK-K8516) in dorsal (A), ventral (B), left lateral (C), and frontal (D) views.

Abbreviations: **a**, angular; **d**, dentary; **ect**, ectopterygoid; **c**, lower canine; **C**, upper canine; **f**, frontal; **fen.m**, mandibular fenestra; **i**, lower incisor; **j**, jugal; **l**, lacrimal; **m**, maxilla; **n**, nasal; **p**, parietal; **part**, prearticular; **pbs**, para-basisphenoid; **PC6**, sixth upper postcanine; **po**, postorbital; **pm**, premaxilla; **prf**, prefrontal; **pt**, pterygoid; **q-qj**, quadrate-quadratojugal complex; **sa**, surangular; **sm**, septomaxilla; **sp**, splenial; **sq**, squamosal; **v.ipt**, interpterygoid vacuity; **v.suborb**, suborbital vacuity.

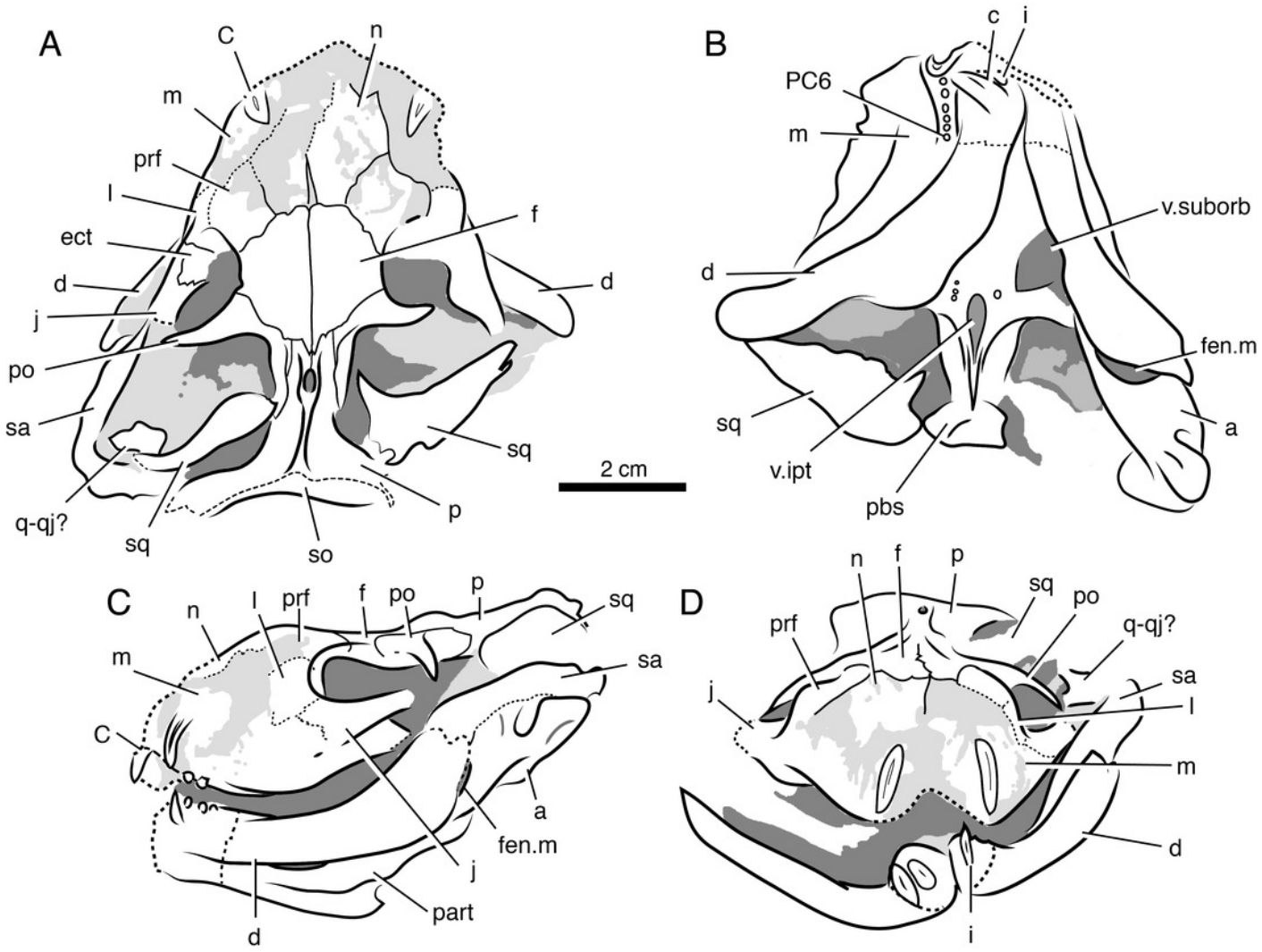

Figure 9

Major clades of eutherocephalians (tree length = 381; consistency index (CI) = 0.438; retention index = 0.789; rescaled CI = 0.346).

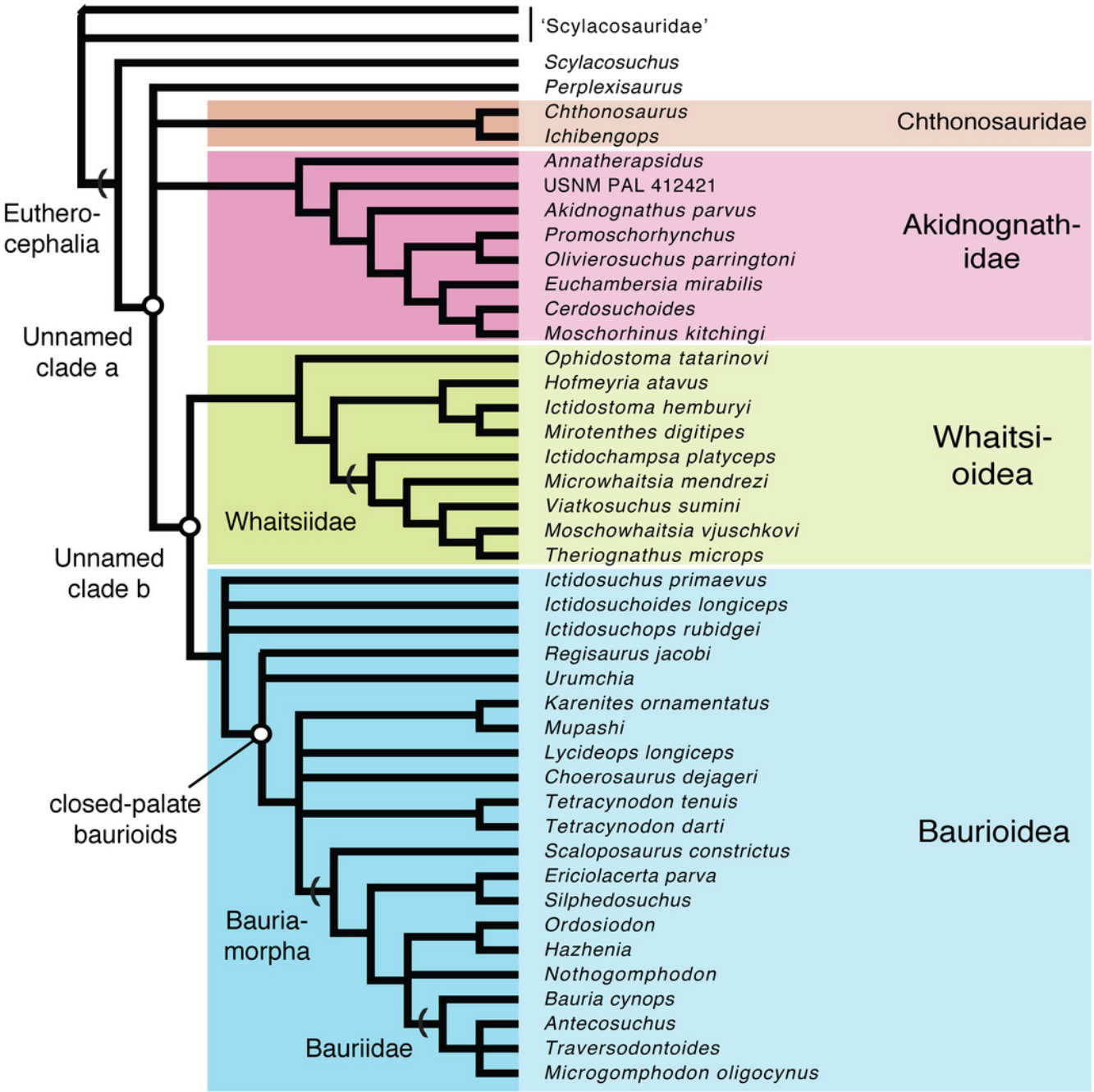

Figure 10

New specimen of the hofmeyriid *Mirotenthes digitipes* Attridge, 1956 (SAM-PKK11188) from the upper *Cistecephalus* Assemblage Zone of 'Good Luck.'

Specimen shown in dorsal oblique view, showing the large temporal fenestra and broad, anvil-shaped epipterygoid (**ept**) processus ascendens.

Figure 11

Stratigraphically calibrated phylogeny of middle Permian through Triassic therocephalians showing calibration points for minimum divergence dates of major clades.

Light gray lines represent hypothetical phylogenetic branching, whereas black bars represent observed stratigraphic ranges (dashed ends indicate taxa having unknown upper or lower ranges). Graph (below) shows peak levels of eutherocephalian origination/extinction by the Wuchiapingian stage. **Abbreviations**: **An**, Antarctica; **Ch**, China; **Chx**, Changxingian; ***Ci*AZ**, *Cistecephalus* Assemblage Zone; ***Dapto*AZ**, *Daptocephalus* Assemblage Zone; **Ind**, Induan; **Na**, Namibia; **Olen**, Olenekian; ***Prist*AZ**, *Pristerognathus* Assemblage Zone; **Roa**, Roadian; **Ru**, Russia; **SA**, South Africa; ***Tapino*AZ**, *Tapinocephalus* Assemblage Zone; ***Tr*AZ**, *Tropidostoma* Assemblage Zone; **Tz**, Tanzania; **Wor**, Wordian; **Za**, Zambia.

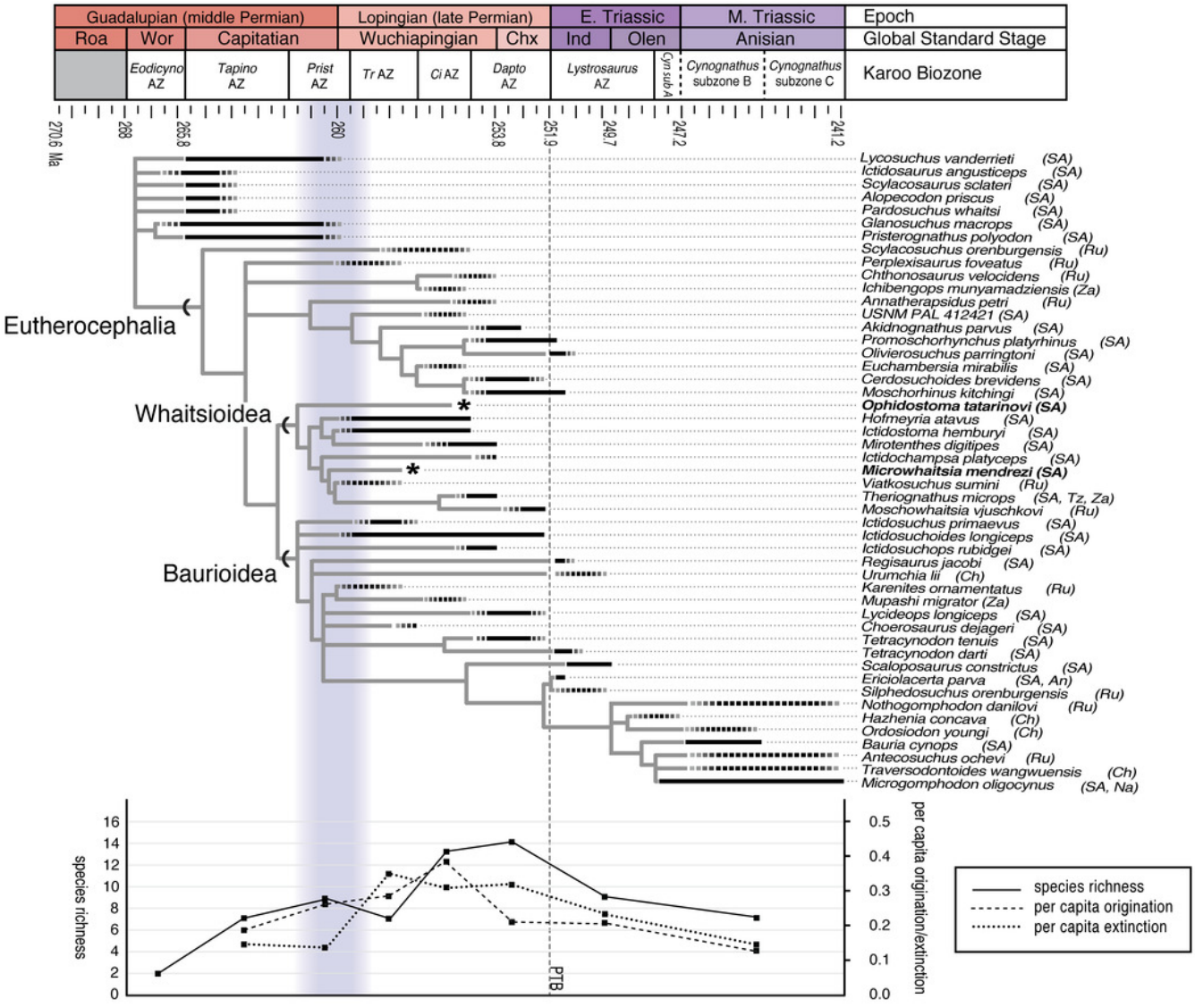
Guadalupian (middle Permian)
Lopingian (late Permian)
E. Triassic
M. Triassic
Epoch
Roa
Wor
Capitatian
Wuchiapingian
Chx
Ind
Olen
Anisian
Global Standard Stage
Eodicyno AZ
Tapino AZ
Prist AZ
Tr AZ
Ci AZ
Dapto AZ
Lystrosaurus AZ
Cyn sub A
Cynognathus subzone B
Cynognathus subzone C
Karoo Biozone
270.6 Ma
268
265.8
260
253.8
251.9
249.7
247.2
241.2
Eutherocephalia
Whaitsioidea
Baurioidea
Lycosuchus vanderrieti (SA)
Ictidosaurus angusticeps (SA)
Scylacosaurus sclateri (SA)
Alopecodon priscus (SA)
Pardosuchus whaitsi (SA)
Glanosuchus macrops (SA)
Pristerognathus polyodon (SA)
Scylacosuchus orenburgensis (Ru)
Perplexisaurus foveatus (Ru)
Chthonosaurus velocidens (Ru)
Ichibengops munyamadziensis (Za)
Annatherapsidus petri (Ru)
USNM PAL 412421 (SA)
Akidnognathus parvus (SA)
Promoschorhynchus platyrhinus (SA)
Olivierosuchus parringtoni (SA)
Euchambersia mirabilis (SA)
Cerdosuchoides brevidens (SA)
Moschorhinus kitchingi (SA)
Ophidostoma tatarinovi (SA)
Hofmeyria atavus (SA)
Ictidostoma hemburyi (SA)
Mirotenthes digitipes (SA)
Ictidochampsa platyceps (SA)
Microwhaitsia mendrezi (SA)
Viatkosuchus sumini (Ru)
Theriognathus microps (SA, Tz, Za)
Moschowhaitsia vjuschkovi (Ru)
Ictidosuchus primaevus (SA)
Ictidosuchoides longiceps (SA)
Ictidosuchops rubidgei (SA)
Regisaurus jacobi (SA)
Urumchia lii (Ch)
Karenites ornamentatus (Ru)
Mupashi migrator (Za)
Lycideops longiceps (SA)
Choerosaurus dejageri (SA)
Tetracynodon tenuis (SA)
Tetracynodon darti (SA)
Scaloposaurus constrictus (SA)
Ericiolacerta parva (SA, An)
Silphedosuchus orenburgensis (Ru)
Nothogomphodon danilovi (Ru)
Hazhenia concava (Ch)
Ordosiodon youngi (Ch)
Bauria cynops (SA)
Antecosuchus ochevi (Ru)
Traversodontoides wangwuensis (Ch)
Microgomphodon oligocynus (SA, Na)
species richness
per capita origination/extinction
PTB
species richness
per capita origination
per capita extinction

Figure 12

Representative hofmeyriid from the late Capitanian or earliest Wuchiapingian of the Karoo Basin, South Africa, compared to other known specimens of *Hofmeyria*.

SAM-PK-K10525 (**A**), Hofmeyriidae from the *Pristerognathus* Assemblage Zone of Lombardskraal, Beaufort West district, Western Cape Province. Specimen shows short, high rostrum, prefrontal-postorbital contact in orbit, anteriorly expanded epipterygoid, and conical, non-serrated/non-carinated maxillary teeth. BP/1/4404 (BP, former Bernard Price Institute, now Evolutionary Studies Institute, Johannesburg) (**B**), *Hofmeyria* cf. *H. atavus* from the *Cistecephalus* Assemblage Zone of Matjiesfontein (Highlands), Victoria West district, Northern Cape Province. BP/1/1399 (**C**), *Hofmeyria* cf. *H. atavus* from the *Cistecephalus* Assemblage Zone of Driehoeksfontein, Murraysburg district, Western Cape Province. Numbers 14–136 are characters listed in the phylogenetic analysis (see online Supplemental Appendix) followed by the derived state in parentheses corresponding to hofmeyriids or other early whaitsioids. **Abbreviations**: **AZ**, Assemblage Zone; **PC**, postcanine position #.

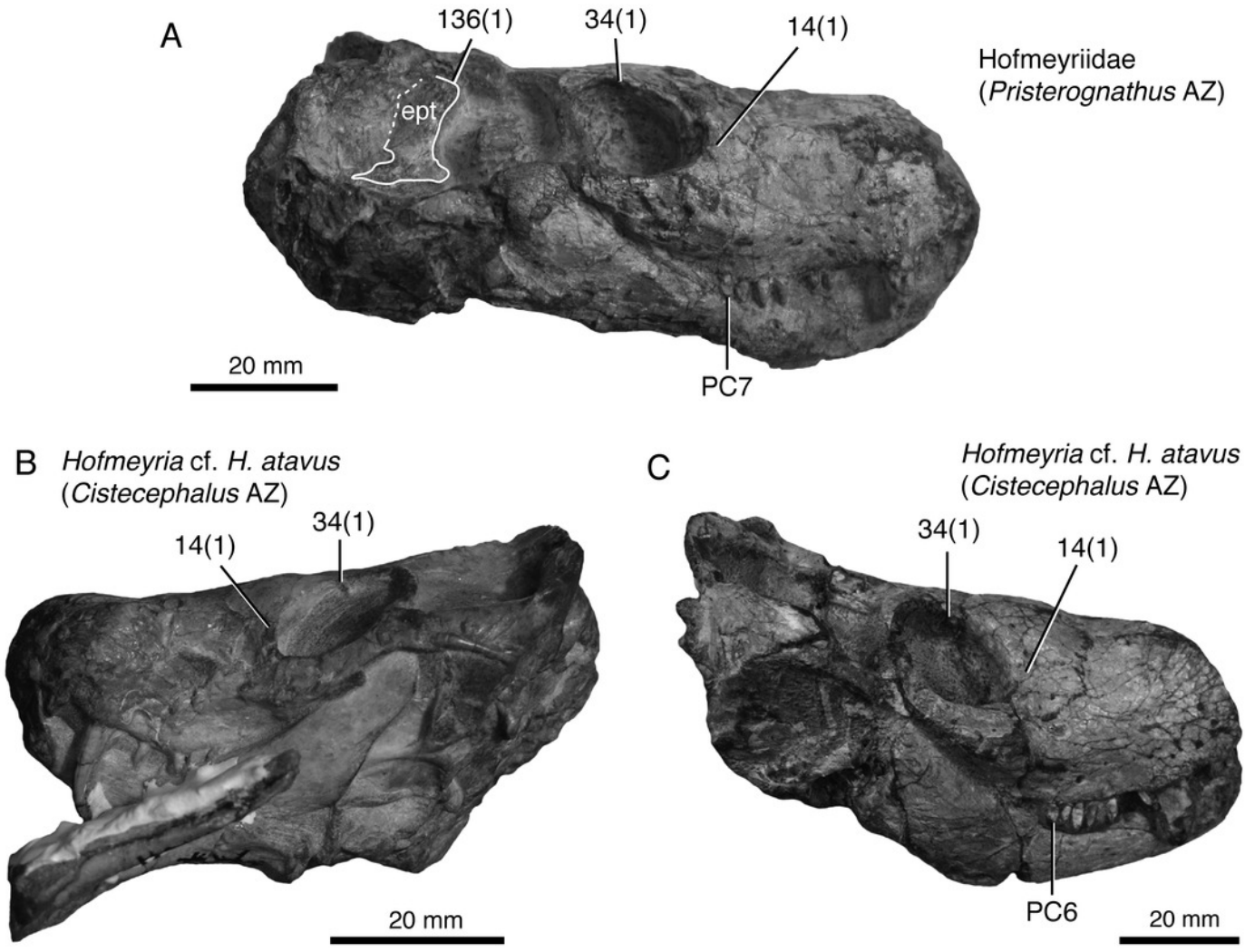
A
136(1)
34(1)
14(1)
ept
Hofmeyriidae
(*Pristerognathus* AZ)
20 mm
PC7
B
Hofmeyria cf. *H. atavus*
(*Cistecephalus* AZ)
14(1)
34(1)
20 mm
C
Hofmeyria cf. *H. atavus*
(*Cistecephalus* AZ)
34(1)
14(1)
PC6
20 mm